

# Cytosolic Hsp60 Is Involved in the NF- $\kappa$ B-Dependent Survival of Cancer Cells via IKK Regulation

Jung Nyeo Chun<sup>1</sup>, Boae Choi<sup>1</sup>, Kyung Wha Lee<sup>1</sup>, Doo Jae Lee<sup>1</sup>, Dong Hoon Kang<sup>1</sup>, Joo Young Lee<sup>1</sup>, In Sung Song<sup>1,2a</sup>, Hye In Kim<sup>1,2b</sup>, Sang-Hee Lee<sup>4</sup>, Hyeon Soo Kim<sup>5</sup>, Na Kyung Lee<sup>1</sup>, Soo Young Lee<sup>1,2</sup>, Kong-Joo Lee<sup>1,3</sup>, Jaesang Kim<sup>1,2</sup>, Sang Won Kang<sup>1,2\*</sup>

**1** Division of Life and Pharmaceutical Science and Center for Cell Signaling and Drug Discovery Research, Ewha Womans University, Seoul, Korea, **2** Department of Life Science and College of Natural Science, Ewha Womans University, Seoul, Korea, **3** College of Pharmacy, Ewha Womans University, Seoul, Korea, **4** Division of Electron Microscopic Research, Korea Basic Science Institute, Daejeon, Korea, **5** Department of Anatomy, College of Medicine, Korea University, Seoul, Korea

## Abstract

Cytoplasmic presence of Hsp60, which is principally a nuclear gene-encoded mitochondrial chaperonin, has frequently been stated, but its role in intracellular signaling is largely unknown. In this study, we demonstrate that the cytosolic Hsp60 promotes the TNF- $\alpha$ -mediated activation of the IKK/NF- $\kappa$ B survival pathway via direct interaction with IKK $\alpha$ / $\beta$  in the cytoplasm. Selective loss or blockade of cytosolic Hsp60 by specific antisense oligonucleotide or neutralizing antibody diminished the IKK/NF- $\kappa$ B activation and the expression of NF- $\kappa$ B target genes, such as Bfl-1/A1 and MnSOD, which thus augmented intracellular ROS production and ASK1-dependent cell death, in response to TNF- $\alpha$ . Conversely, the ectopic expression of cytosol-targeted Hsp60 enhanced IKK/NF- $\kappa$ B activation. Mechanistically, the cytosolic Hsp60 enhanced IKK activation via upregulating the activation-dependent serine phosphorylation in a chaperone-independent manner. Furthermore, transgenic mouse study showed that the cytosolic Hsp60 suppressed hepatic cell death induced by diethylnitrosamine *in vivo*. The cytosolic Hsp60 is likely to be a regulatory component of IKK complex and it implicates the first mitochondrial factor that regulates cell survival via NF- $\kappa$ B pathway.

**Citation:** Chun JN, Choi B, Lee KW, Lee DJ, Kang DH, et al. (2010) Cytosolic Hsp60 Is Involved in the NF- $\kappa$ B-Dependent Survival of Cancer Cells via IKK Regulation. PLoS ONE 5(3): e9422. doi:10.1371/journal.pone.0009422

**Editor:** Rafael Linden, Universidade Federal do Rio de Janeiro (UFRJ), Brazil

**Received:** December 2, 2009; **Accepted:** January 18, 2010; **Published:** March 23, 2010

**Copyright:** © 2010 Chun et al. This is an open-access article distributed under the terms of the Creative Commons Attribution License, which permits unrestricted use, distribution, and reproduction in any medium, provided the original author and source are credited.

**Funding:** This study was supported by 21C Frontier Functional Proteomics Project (FPR08-B1-190) funded by the Ministry of Education, Science & Technology and by KOSEF through the Center for Cell Signaling & Drug Discovery Research (CCS & DDR, R15-2006-020) at Ewha Womans University. This study was also supported in part by a grant of the National R&D Program for Cancer Control, Ministry of Health & Welfare (0420190). J. N. Chun, K. W. Lee, J. Y. Lee, B. A. Choi, and H. I. Kim were supported by Brain Korea 21 grant from the Korea Ministry of Education, Science & Technology. The funders had no role in study design, data collection and analysis, decision to publish, or preparation of the manuscript.

**Competing Interests:** The authors have declared that no competing interests exist.

\* E-mail: kangsw@ewha.ac.kr

<sup>2a</sup> Current address: Medical Genomics Research Center, Korea Research Institute of Bioscience and Biotechnology, Daejeon, Korea

<sup>2b</sup> Current address: CMP Korea Medica Ltd. Seoul, Korea

## Introduction

Mammalian cells express a number of survival genes that play the roles in inhibiting caspase activation, removing harmful oxygen radicals, defending mitochondrial function, and checking cell cycle. Among the transcription factors responsible for the induction of the survival genes, nuclear factor- $\kappa$ B (NF- $\kappa$ B) is a key element that orchestrates the complex cell survival response [1]. In particular, the NF- $\kappa$ B-dependent survival genes include anti-apoptotic genes, such as c-IAPs and c-FLIP, and mitochondrial safeguard genes, such as manganese-superoxide dismutase (MnSOD) and Bcl-2 family members [2,3,4]. A central kinase in NF- $\kappa$ B activation pathway is the inhibitor of  $\kappa$ B kinase (I $\kappa$ B kinase or IKK) that phosphorylates the I $\kappa$ B protein in two amino-terminal serine residues, leading to its ubiquitinylation and proteosomal degradation and to the consequent liberation of NF- $\kappa$ B proteins [5]. The extracellular stimuli to activate NF- $\kappa$ B pathway converge to IKK [6]. Therefore, numerous efforts have been made to delineate the regulation of IKK activation. First, the phosphorylation-dependent regulation of IKK activation has been characterized [7]. The phosphorylation of two serine residues (Ser

177/Ser181 in human IKK $\beta$ ) in activation T-loop is essential for activation, while the autophosphorylation of carboxyl-terminal serine cluster turns off the activation. Many kinases have been implicated to be involved in the activation phosphorylation: NF- $\kappa$ B-inducing kinase (NIK) [8,9], mitogen-activated protein kinase/ERK kinase kinases 1 (MEKK1) [10], MEKK2/3 [11,12], Hematopoietic progenitor kinase-1 (HPK1) [13], Mixed-lineage kinase 3 (MLK3) [14], TGF- $\beta$  activated kinase 1 (TAK1) [15]. However, except TAK1, it is unclear how the upstream kinase activates the IKK complex. Second, the ubiquitin-dependent regulation of IKK activation has been studied for many years [15,16]. Recently, the regulatory subunit IKK $\gamma$  (or NEMO) of IKK complex has been shown to be ubiquitinated, as well as to recognize Lys63-linked polyubiquitination chain on receptor-interaction protein 1 (RIP1) [17,18]. Thirdly, the regulation of IKK activation via the interacting proteins has been characterized. The best examples are heat shock proteins. For example, Cdc37 and Hsp90 have been reported to act as additional components of the IKK complex that stabilize the complex [19,20]. Hsp27 has been shown to interact with IKK $\beta$  in a TNF- $\alpha$ -dependent manner [21]. Hsp70 also interacts with IKK $\gamma$  but interferes with the IKK

activation [22]. Besides, the association between protein phosphatase 2C $\beta$  (PP2C $\beta$ ) and the IKK complex has been demonstrated [23], and ELKS has also been identified as a new regulatory subunit of IKK complex that mediates the recruitment of I $\kappa$ B to the complex [24]. However, there is no indication of a mitochondrial protein involved in the IKK/NF- $\kappa$ B activation.

We have recently identified heat shock protein 60 (Hsp60) as an IKK-interacting protein. Hsp60 is the mitochondrial chaperonin that promotes the folding of the imported protein to native conformation. Nonetheless, the existence and function of Hsp60 in extramitochondrial compartments has frequently been stated [25]. For example, Hsp60 can be a ligand for cell-surface receptors like toll-like receptor [26]. Intracellularly, Hsp60 has been shown to interact with pro-caspase-3 or Bax [27,28,29]. However, the function of Hsp60 related to cell survival signaling has not been reported. In this study, Hsp60 was found to mediate the NF- $\kappa$ B-dependent survival signaling in the cells. Specifically, Hsp60 directly interacted with IKK $\alpha$ / $\beta$  in cytoplasm and then promoted the phosphorylation-dependent activation of the kinase in response to TNF- $\alpha$ . Such signaling function of Hsp60 was independent of its chaperone activity, which sets Hsp60 apart from other heat shock proteins that function via stabilizing or destabilizing signaling complex [30]. We also showed *in vivo* evidence that cytosolic expression of Hsp60 protects hepatic cells against chemical-induced damages via enhancing IKK activation. Thus, this finding represents the novel pro-survival function of cytosolic Hsp60 and shed a light on understanding the function of Hsp60 in extra-mitochondrial compartments [25].

## Results

### Hsp60 interacts with IKK complex in cytoplasm

To identify an additional component, we examined the molecular composition of the latent IKK complex using a proteomic technique combining immuno-affinity purification and mass spectrometry. Briefly, the IKK complex was precipitated from the lysates of unstimulated HeLa S3 cells using anti-IKK $\alpha$  antibody beads, and the co-precipitated proteins were sequenced by liquid chromatography-tandem mass spectrometry. The identification of the IKK subunits and Hsp90 indicated that the immunoprecipitation of IKK complex fairly worked (Fig. 1A). As a consequence, this proteomic study identified a heat shock protein, Hsp60, in the precipitates (Fig. 1A and 1B). The presence of the IKK subunits and Hsp60 in the precipitates was confirmed by immunoblotting (Fig. 1C). Then, we decided to investigate the biological meaning of the IKK-Hsp60 interaction.

The first step was to verify the endogenous interaction of Hsp60 and IKKs by co-immunoprecipitation experiments. When the heterogeneous IKK complexes were precipitated with antibodies against IKK $\alpha$ , IKK $\beta$ , and IKK $\gamma$ , each of the IKK subunit-specific antibodies similarly precipitated Hsp60 (Fig. 1D). In addition, Hsp90 was also co-precipitated with IKK complex [20,21]. This interaction was found to be unaffected by TNF- $\alpha$  treatment (Fig. 1E), indicating that Hsp60 is a component protein of heterogeneous IKK complexes. A reverse immunoprecipitation was then carried out with the cytosolic fraction to exclude the mitochondrial contamination. The anti-Hsp60 antibodies co-precipitated IKK $\gamma$  with Hsp60, whereas control goat IgG did not (Fig. 1F), confirming that cytosolic interaction of Hsp60 and IKK. In order to visualize the virtual interaction of Hsp60 with IKKs in cytoplasm, the immunogold staining combined with the electron microscopy (EM) was performed. The immune complexes of Hsp60 and IKK with their specific antibodies were detected differently using secondary antibodies labeled with 20 nm-

40 nm-diameter gold particles, respectively. As a result, the Hsp60-labeling gold particles were distributed throughout the cellular structures: not only in the matrix and intermembrane space of mitochondria, but also in the cytoplasm and plasma membrane (Fig. 2B). In contrast, the IKK $\alpha$ - and IKK $\beta$ -labeling gold particles were mainly detected in the cytoplasm (Fig. 2C and 2D), while the IKK $\alpha$  was also detected in the nucleus, which is consistent with the previous reports [31,32]. Although the IKK core subunits have been shown to be found in the mitochondrial fraction [33], our data showed that the IKK-labeling gold particles were often seen in the vesicular structures rather than the mitochondria (Fig. 2C and 2D). This discrepancy might be due to the previous study done with subcellular fractionation. When the Hsp60 and IKKs were co-stained, the direct binding of 20 nm and 40 nm gold particles was clearly detected in the cytoplasm (Fig. 2E and 2F). It should be noted that not all of the IKK $\alpha$  and IKK $\beta$  were associated with Hsp60. These results collectively indicate that the Hsp60 directly interacts with IKK complex in the cytosol.

### Hsp60 directly interact with IKK $\alpha$ / $\beta$ , not IKK $\gamma$

Next, we analyzed the molecular interaction of Hsp60 and IKKs. To do this, a cytosol-targeted version of Hsp60 (Hsp60c), wherein the mitochondrial targeting signal sequence is deleted, was constructed. When Hsp60c was co-expressed with each of the IKK core subunits, Hsp60c interacted with IKK $\alpha$  and, albeit to a lesser extent, with IKK $\beta$ , but not with IKK $\gamma$  (Fig. 3A). Then, an *in vitro* binding experiment using the recombinant proteins of glutathione-S-transferase (GST)-fused Hsp60 and (His)<sub>6</sub>-tagged IKK core subunits was assessed by a GST pull-down assay. The result, again, indicates that Hsp60 binds directly to IKK $\alpha$  and IKK $\beta$ , but not to IKK $\gamma$  (Fig. 3B).

The molecular interaction of Hsp60 with IKK was further characterized by domain mapping experiments. Because the C-terminal deletion hampered the ectopic expression, a series of N-terminal deletion mutants of Hsp60c was tested for IKK binding via co-expression with Flag-tagged IKK $\alpha$  in HEK293 cells (Fig. 3C). The results showed that the N-terminal part (~160 amino acids from N-terminus) of Hsp60 protein was shown to be dispensable for the interaction (Fig. 3D). The same result was obtained when endogenous IKK complex was immunoprecipitated from HeLa cells transfected with the Hsp60c constructs (Fig. 3E). The results fairly indicate that the core binding domain is located in the middle of Hsp60 protein.

### Hsp60 is involved in the IKK/NF- $\kappa$ B activation

Next, the biological effect of cytosolic Hsp60-IKK interaction was investigated in TNF- $\alpha$ -mediated NF- $\kappa$ B pathway. To achieve the goal, the essential step is to manipulate the level of cytosolic Hsp60 without affecting the mitochondrial one because Hsp60 deficiency is known to cause a mitochondrial functional defect [34,35,36]. Interestingly, a number of studies has previously reported that an antisense oligodeoxynucleotide (AS-ODN) complementary to a sequence surrounding the start codon of the human Hsp60 open reading frame actually reduces the cytosolic Hsp60 level [27,37,38]. We, therefore, decided to test this AS-ODN (designated as AS-1) for a selective knockdown effect. In order to exclude the possibility of non-specific action of a particular ODN sequence, we chose a second AS-ODN (AS-2) that is complementary to the region (+95~+110 from start codon) near the 5' end, but after mitochondrial targeting signal sequence (MTS), of Hsp60 open reading frame (Fig. S1A). The sense ODN (S-ODN) complementary to AS-1 was used as a control ODN. Since the antisense ODN is a moderate

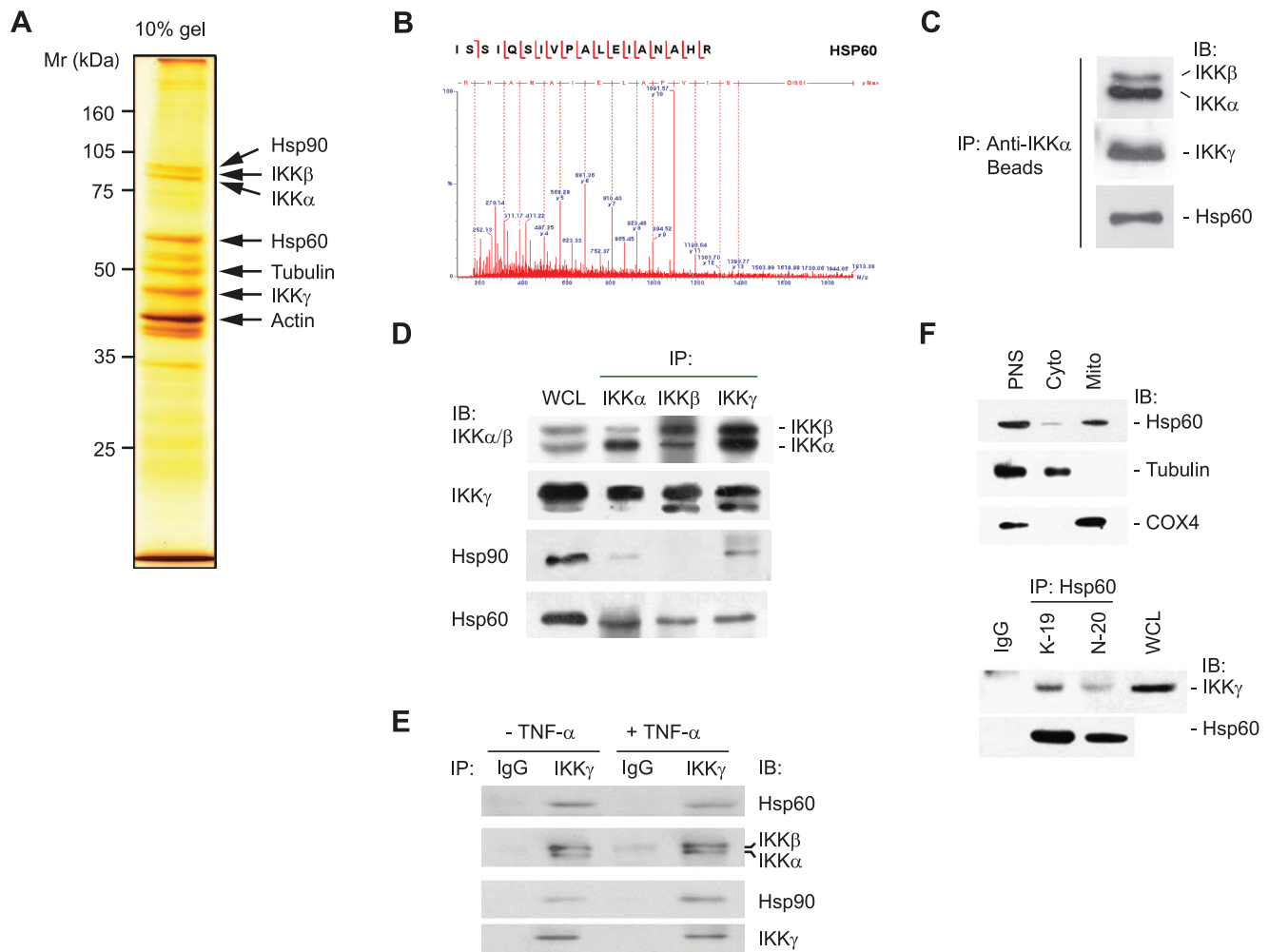


**Figure 1. Identification of Hsp60 in IKK complex.** **A.** A silver-stained polyacrylamide gel resolving the affinity-purified IKK complex. **B.** MS/MS spectra of  $[M+2H]^{2+}$  ions of the peptides derived from the protein band corresponding to Hsp60. **C.** Immunoblot (IB) analyses of IKK subunits and Hsp60 in the affinity-purified complex. **D.** Interaction of Hsp60 with IKK complex. IKK complex was immunoprecipitated (IP) from HeLa cell lysates (500  $\mu$ g total proteins for each) with IKK $\alpha$ , IKK $\beta$ , and IKK $\gamma$ -specific antibodies. The IKK $\alpha$ / $\beta$ / $\gamma$  subunits, Hsp60, and Hsp90 were immunoblotted. WCL, whole cell lysate. **E.** TNF- $\alpha$ -independent interaction of Hsp60 and IKK complex. **F.** Co-immunoprecipitation of Hsp60 and IKK complex in cytosolic fraction. *Upper panel*, post-nuclear supernatant (PNS), cytosol (Cyto), and mitochondria (Mito) fractions from HeLa cells were immunoblotted. COX4 and tubulin were used as mitochondrial and cytosolic markers, respectively. *Lower panel*, Hsp60 was immunoprecipitated from the cytosolic fraction using either control goat IgG or anti-Hsp60 antibodies (K-19 and N-20). Representative blots are shown ( $n = 3$ ). doi:10.1371/journal.pone.0009422.g001

translational blocker, it did not elicit the reduction of total Hsp60 level (Fig. S1B). However, the transfection of AS-ODNs indeed selectively reduced cytosolic Hsp60 levels compared to the mock or control S-ODN without affecting the mitochondrial level (Fig. 4A). To understand this phenomenon, we hypothesized that the half-life of Hsp60 protein in two compartments may differ. To prove it, the half-life of cytosol-targeted Hsp60 (Hsp60c) was assessed after inhibition of protein synthesis. Surprisingly, the level of cytosolic Hsp60 protein was rapidly reduced (calculated  $t_{1/2} = 3.2$  min), while total level of endogenous Hsp60 and IKK $\alpha$  proteins was unchanged (Fig. 4B). Moreover, this reduction was completely blocked by the treatment of a proteasome inhibitor MG132 (Fig. 4C). It is noted that the MG132 treatment also resulted in the remarkable increase of the basal level of the Hsp60c protein. Thus, this result, at least in part, explains why the level of cytosolic Hsp60 was more sensitive to AS-ODN treatment, and it additionally suggests that the level of cytosolic Hsp60 might be controlled by proteasome.

The TNF- $\alpha$ -induced IKK/NF- $\kappa$ B activation was then examined in the AS-ODN-transfected cells. An *in vitro* kinase assay showed that the transfection of AS-ODNs appreciably reduced the IKK activation in response to TNF- $\alpha$  by 60% compared to that of the mock or S-ODN (Fig. 4D). However, the AS-ODNs had no effect on the MAP kinase activation in response to TNF- $\alpha$  (Fig. 4D and Fig. S1C), revealing the specific effect of the Hsp60 AS-ODNs on IKK activation. Furthermore, the AS-ODNs almost completely abolished the NF- $\kappa$ B transcriptional activation in response to TNF- $\alpha$ , whereas S-ODN did not, compared to mock-treated cells (Fig. 4E). Owing to its knockdown efficacy, AS-1 is more potent than AS-2. However, the transfection of ODNs itself did not induce basal NF- $\kappa$ B activation, indicating no off-target effect of ODNs. In addition, the reductive effect of AS-ODNs on NF- $\kappa$ B transcriptional activity was also evident in 293T and A549 cells (Fig. S1D). An additional control experiment showed that the AS-ODNs had no effect on other transcription factor activation, such as AP-1, NF-AT, and CRE (Fig. S1E).

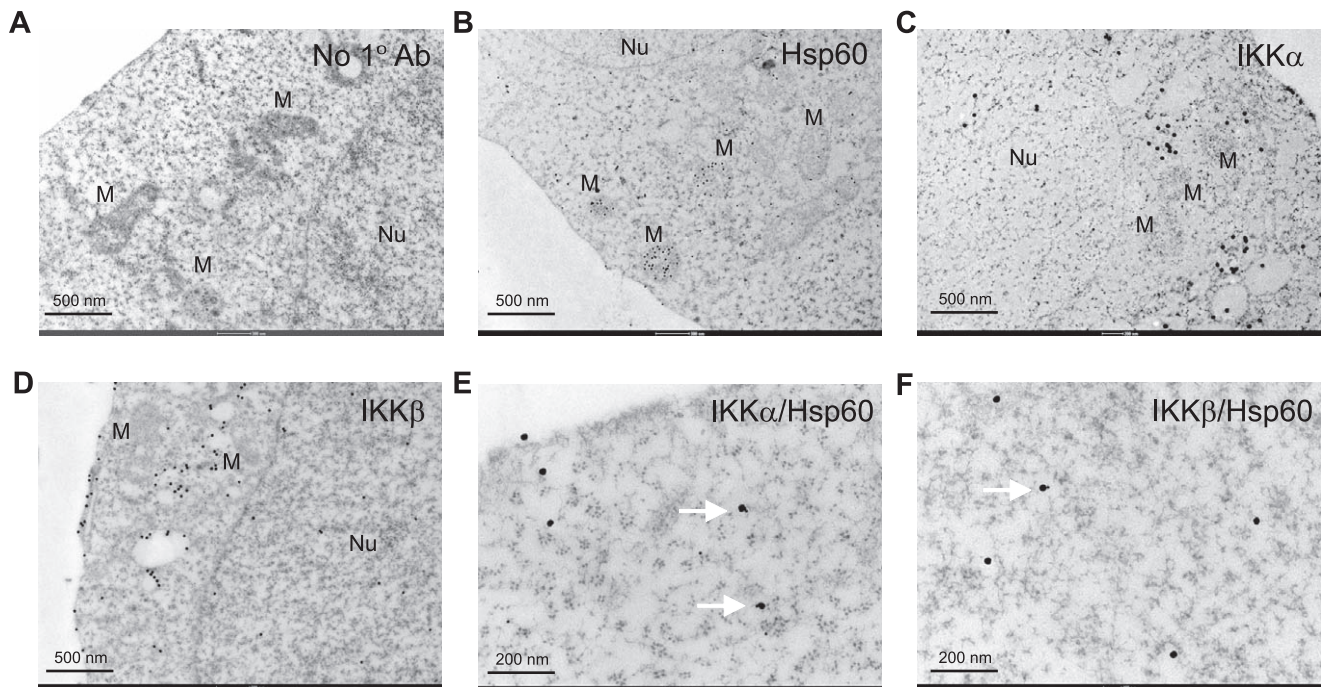


**Figure 2. Visualization of Hsp60 and IKK interaction at a single-cell level.** HeLa cells were immunoreacted with no primary (A), anti-Hsp60 (B), anti-IKK $\alpha$  (C), anti-IKK $\beta$  (D), anti-Hsp60/IKK $\alpha$  (E), and anti-Hsp60/IKK $\beta$  (F) antibodies, and then labeled with the corresponding secondary antibodies conjugated with 20 nm or 40 nm gold particles, as described in Experimental Procedure. The labeling was assessed by immuno-gold electron microscopy. Nuclei (Nu) and mitochondria (M) are indicated. Arrows indicate direct adherence of Hsp60- and IKK-labeled gold particles. No immunoreactive signal was seen in the sample without primary antibodies (A). The experiments were repeated twice with the same results, and representative results are shown.

doi:10.1371/journal.pone.0009422.g002

A similar study was performed by blocking the cytosolic Hsp60 using a specific antibody (Hsp60N), which has been used for immunoprecipitation and immunostaining of Hsp60 (see Fig. 1). The antibody transduction was achieved by a peptide-mediated protein delivery system [39]. The control goat IgG and Hsp60N antibody were found to be successfully delivered to cytoplasm, as being not merged with Mitotracker (Fig. 5A), and Hsp60N, but not control IgG, bound to Hsp60 (Fig. 5B). This result indicates that the delivered antibody can act as a function blocker. Then, IKK/NF- $\kappa$ B activation was examined in antibody-transduced cells. The Hsp60N antibody evidently reduced the IKK activation in response to TNF- $\alpha$  by 50% of the level obtained with the control IgG (Fig. 5C). In contrast, TNF- $\alpha$ -induced JNK activation was not affected, which again proves that the role of Hsp60 is specific to the IKK activation. Consistently, the Hsp60N antibody significantly reduced the transcriptional activity of NF- $\kappa$ B (Fig. 5D). The data collectively conclude that cytosolic Hsp60 promotes the TNF- $\alpha$ -induced IKK/NF- $\kappa$ B signaling.

#### Ectopic expression of cytosol-targeted Hsp60 sufficiently promotes IKK/NF- $\kappa$ B activation

Conversely, the role of cytosolic Hsp60 in IKK/NF- $\kappa$ B pathway was addressed by over-expression of cytosol-targeted Hsp60c. The ectopically-expressed Hsp60c was found to associate with the IKK complex (Fig. 6A) and markedly enhanced the IKK and NF- $\kappa$ B activation in response to TNF- $\alpha$  (Fig. 6B and 6C). It should be noted that the ectopic expression of Hsp60c marginally induced the basal IKK and NF- $\kappa$ B activation. The effect of Hsp60c expression in NF- $\kappa$ B activation was completely abolished in IKK $\beta$ -deficient cells (Fig. 6D), indicating that the regulatory

activity of cytosolic Hsp60 is IKK-dependent. In addition, the ectopic expression of Hsp60c did not enhance either JNK activation or the activation of other transcription factors such as AP-1, CRE, and NF-AT (Fig. S2). This result indicates that increasing the cytosolic Hsp60 level augments TNF- $\alpha$ -induced IKK/NF- $\kappa$ B activation.

#### Hsp60 regulates IKK phosphorylation at the activation T-loop

To understand the mechanism underlying the regulatory action of Hsp60 in IKK/NF- $\kappa$ B activation, several experimental approaches were attempted. To determine whether the chaperone activity of Hsp60 is required, the two amino acid residues that are known to be critical for the chaperone activity of Hsp60 were considered. One is a lysine residue (K28), which is involved in the oligomerization of Hsp60 protein [40,41]. The other is an aspartate residue (D423), which is an active site residue for ATPase activity [42,43]. Thus, the Hsp60c mutants, wherein K28 and D423 are substituted with glutamate and alanine respectively, were constructed. The co-transfection experiment showed that both mutants interacted with IKK $\alpha$  and IKK $\beta$  as well as or perhaps even better than the wild type (Fig. 7A). The IKK activation in response to TNF- $\alpha$  in the Hsp60 mutant-expressing cells was similar to that in the wild type (Fig. 7B), indicating that such loss-of-function mutations did not affect the IKK-enhancing activity. Furthermore, TNF- $\alpha$ -induced NF- $\kappa$ B transcription was even enhanced in the Hsp60 mutant-expressing cells at approximately 4–6 times higher than that in the vector control (Fig. 7C). The enhancing effect of the mutants was clearly IKK $\beta$ -dependent, as tested again in IKK $\beta$ -deficient 3T3 cells. Thus, this experiment

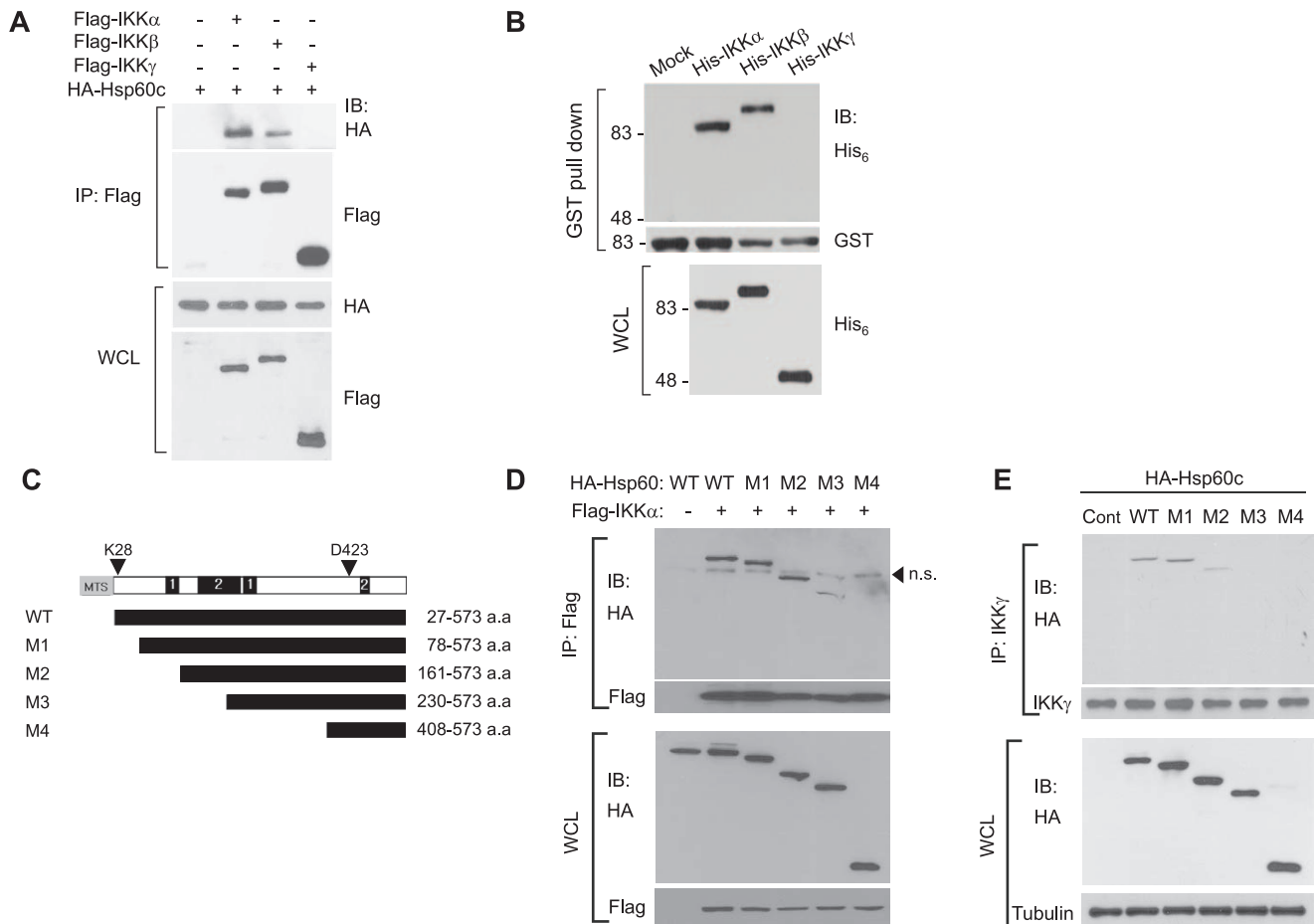


**Figure 3. Hsp60 directly interacts with IKK complex.** **A.** Direct binding of Hsp60 and IKK subunits. The 293T cells were co-transfected with Hsp60c (HA tag) and each of IKK subunit proteins (Flag tag) for 24 hrs. **B.** *In vitro* association of Hsp60 with IKK $\alpha$  and IKK $\beta$ . GST-fused Hsp60 proteins bound to the glutathione Sepharose beads was incubated with the lysates of Sf9 insect cells expressing His<sub>6</sub>-tagged IKK proteins. Hsp60 and IKKs were detected by immunoblotting for GST and HA tags, respectively. **C.** Schematic diagram showing deletion mutants of Hsp60. The putative phosphorylation sites of kinases, including PKA/PKG (1) and PKC (2), are indicated. **D** and **E.** Interaction of Hsp60 wild-type (WT) and deletion mutants with ectopically-expressed IKK $\alpha$  in 293T cells (**D**) or to endogenous IKK complex in HeLa cells (**E**). The control vector (C) is indicated. Representative blots and images are shown ( $n=3$ ). n.s., nonspecific. doi:10.1371/journal.pone.0009422.g003

using the loss-of-function mutants strongly suggest that the cytosolic Hsp60 functions independently of chaperone activity in IKK/NF- $\kappa$ B activation.

One of the IKK-interacting protein, ELKS, has been shown to mediate the I $\kappa$ B recruitment to IKK complex [24]. To test this mode of action, the recombinant Hsp60 protein was directly added into the IKK kinase reaction, where the activated IKK complex is incubated with full-length human I $\kappa$ B as a substrate. The *in vitro* kinase activity of the activated IKK toward I $\kappa$ B was not affected by the presence of Hsp60 protein (Fig. 7D), indicating that Hsp60 is not involved in the interaction of IKK and its substrate I $\kappa$ B.

Lastly, a direct involvement of cytosolic Hsp60 in IKK activation was addressed by examining the activation-dependent serine phosphorylation in the T-loop of IKK $\alpha$ / $\beta$ . The AS-ODN transfection markedly abolished the TNF- $\alpha$ -induced phosphorylation of IKK at Ser178/181, indicating that the phosphorylation-dependent IKK activation was impaired (Fig. 7E). Conversely, the ectopic expression of Hsp60c resulted in an increase of IKK phosphorylation (Fig. 7F). Overall, the data indicate that the cytosolic Hsp60 is involved in the phosphorylation-dependent

IKK activation, rather than the chaperone-dependent stabilization of IKK complex.

### Cytosolic Hsp60 affects the NF- $\kappa$ B target gene expression and cell survival

To determine the significance of cytosolic Hsp60-mediated regulation of the IKK/NF- $\kappa$ B pathway, we examined the expression of NF- $\kappa$ B target genes in ODN-transfected cells. When the expression of anti-apoptotic genes was screened by a RNase protection assay [44], the expression of TRAF1, c-IAP1, and c-IAP2 were not affected by AS-ODN transfection (Fig. 8A). This was unexpected but led us to postulate a possibility that some select target genes related to mitochondrial protection can be affected. To test this, we looked at the induction of several target genes, including antioxidant proteins (ferritin heavy chain and MnSOD) and Bcl-2 members (Bcl-2, Bcl-X<sub>L</sub>, Bfl-1/A1). Interestingly, the AS-ODN significantly diminished the induction of only MnSOD and Bfl-1/A1 expression in response to TNF- $\alpha$  (Fig. 8B). The Hsp60N antibody also significantly reduced the induction of these genes (Fig. 8C). It was again confirmed that the induction of the c-IAP2 expression was not affected in either case. Thus, the results

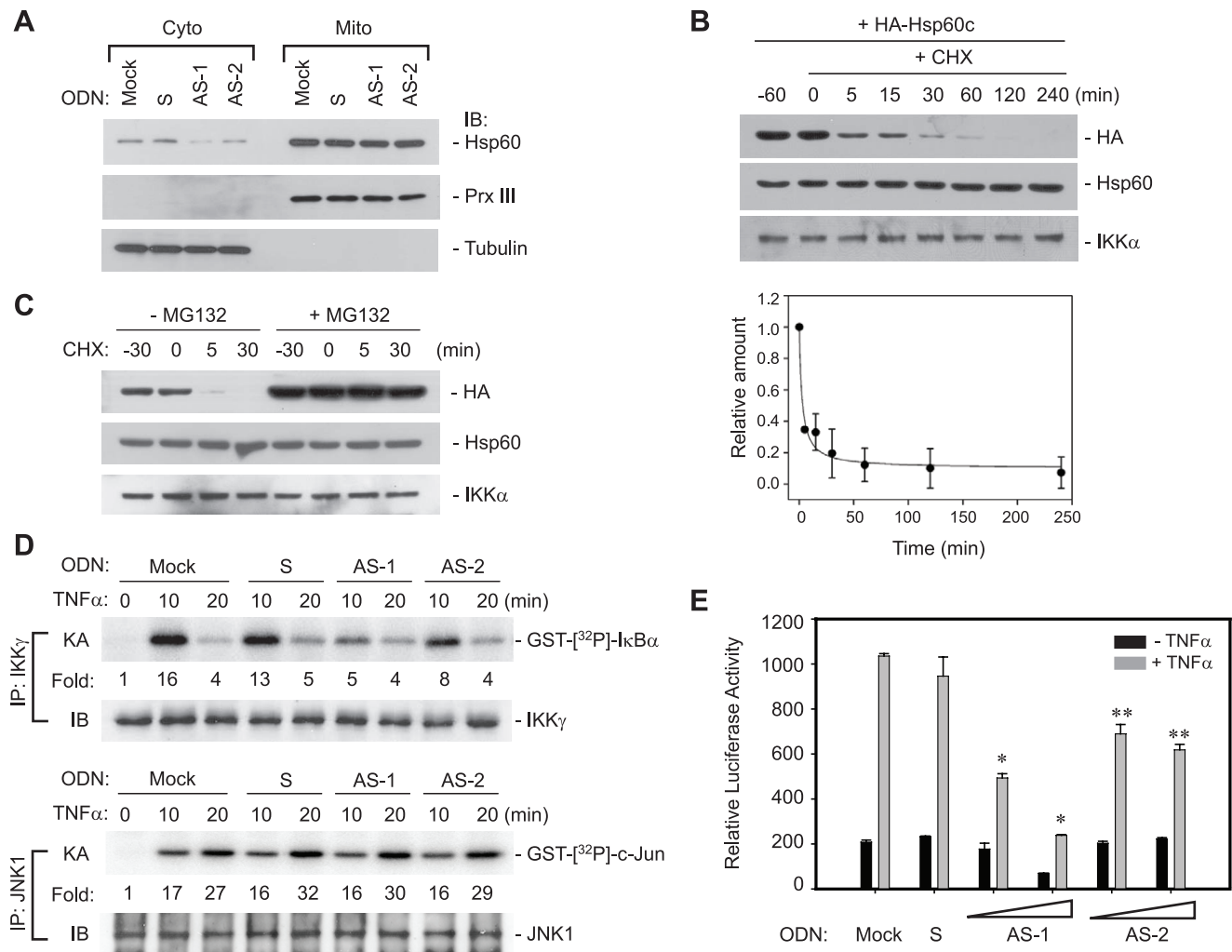


**Figure 4. Loss of cytosolic Hsp60 diminishes IKK/NF- $\kappa$ B activation in response to TNF- $\alpha$ .** **A.** Ablation of cytosolic Hsp60 by antisense ODNs. The cytosolic and mitochondrial fractions prepared from mock or ODN-transfected HeLa cells were immunoblotted. S, sense ODN; AS-1 and AS-2, antisense ODNs. The mitochondrial fraction was loaded at a volume of one-fifth of the corresponding cytosolic fraction. In particular, Prx III, which is an antioxidant enzyme present in the mitochondrial matrix, was used as mitochondrial markers to watch the nonspecific mitochondrial rupture. **B.** Half-life of ectopically-expressed Hsp60c protein (HA tag) after inhibition of protein synthesis with cycloheximide. The intensity of HA band was measured and normalized by the amount of IKK $\alpha$  band. Data in the graph are means  $\pm$  S.D. of two independent experiments and fitted in SigmaPlot 8.0 software. **C.** Proteasome-dependent turnover of cytosolic Hsp60c protein. HeLa cells were pretreated with or without MG132 (5  $\mu$ M) 30 min before cycloheximide treatment. **D.** TNF- $\alpha$ -induced IKK and JNK1 activation in mock or ODN-transfected cells. The *in vitro* kinase activity (KA) was averaged with the values from two independent experiments, and it is represented as a fold increase of the activity versus the unstimulated and mock-transfected cells (lane 1). **E.** NF- $\kappa$ B transcriptional activation in mock or ODN-transfected cells. The increasing concentration of AS-ODN (100 nM or 200 nM) was tested. The relative luciferase activity was normalized to the  $\beta$ -galactosidase activity and data are means  $\pm$  S.D. of four independent experiments (\* $P$ <0.0001, \*\* $P$ <0.001 versus stimulated S-ODN-transfected cells). doi:10.1371/journal.pone.0009422.g004

indicate that the regulation of the IKK activation by cytosolic Hsp60 influences the expression of select NF- $\kappa$ B target genes.

We next wondered whether such regulation of select target genes has an impact on cell survival. Since there is a possibility that MnSOD and Bif-1/A1 function to suppress the mitochondrial-derived reactive oxygen species (ROS) [2,45], the level of cellular ROS was examined in ODN-transfected cells using an oxidation-sensitive fluorescence dye, CM-H<sub>2</sub>DCFDA. The AS-ODN transfection induced a marked increase of cellular ROS in response to TNF- $\alpha$  treatment in a time-dependent manner, compared to mock or S-ODN transfection (Fig. 8D). Since the enhanced ROS level is linked to cell death via the sustained JNK activation [46], the sustained activation of stress-activated protein kinases, JNK and p38 MAPK, was examined. Unexpectedly, the

activation of both JNK and p38 MAPK were found to be clearly sustained in AS-ODN-transfected cells (Fig. 8E). The ASK-1 MAP3K is known to be responsible for the sustained activation of JNK and p38 in the ROS-mediated cell death [47]. Indeed, the ASK-1 activation was significantly induced in AS-ODN-transfected cells (Fig. 8F). As a consequence of this signaling pathway including ASK-1 activation, the AS-ODN resulted in a marked induction of TNF- $\alpha$ -induced cell death in HeLa cells, whereas the mock or S-ODN did not at all (Fig. 8G). Likewise, the AS-ODN enhanced TNF- $\alpha$ -induced cell death in colon carcinoma cell lines, which showed significant level of cytosolic Hsp60 (Fig. 8H). It should be noted that the AS-ODN transfection by itself resulted in the basal activation of ROS, ASK1, and cell death. Along with the evidence that the Hsp60c overexpression induced the basal IKK/

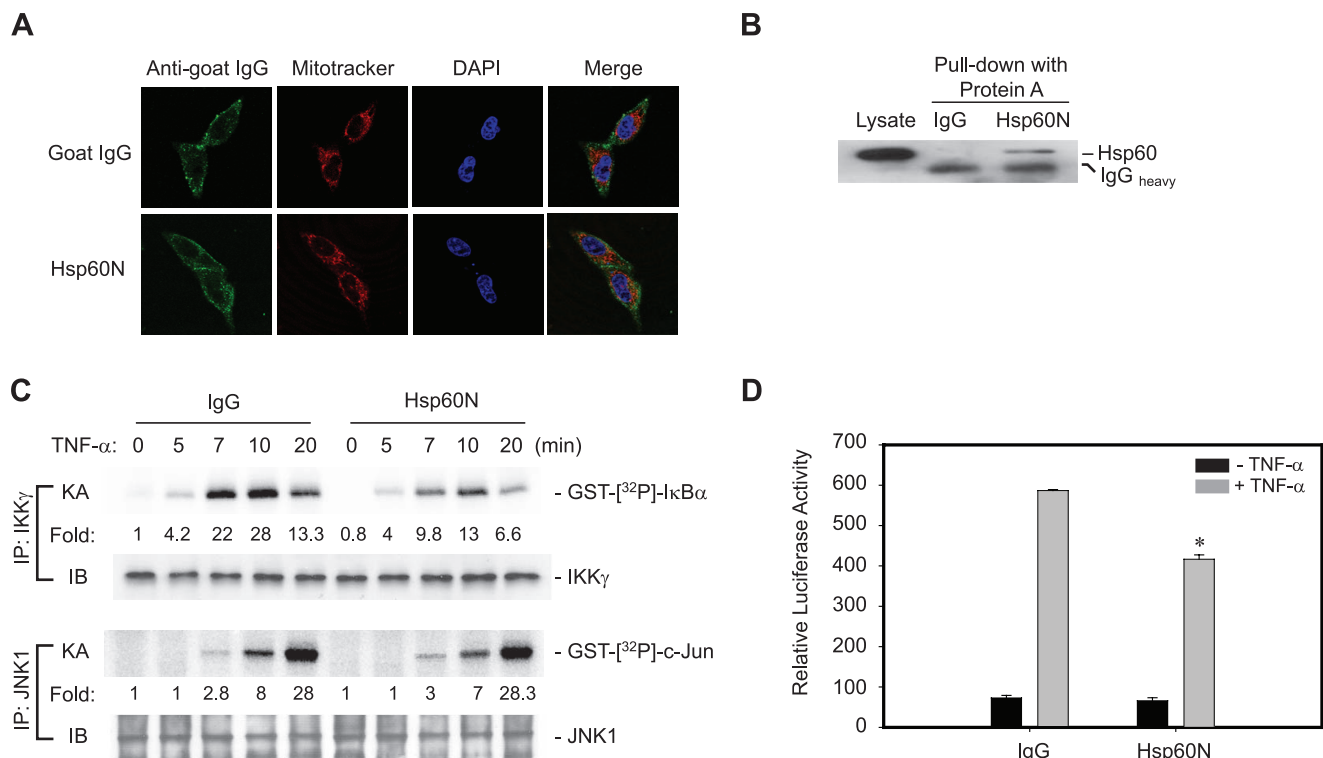


**Figure 5. Hsp60-specific antibody blocks IKK/NF- $\kappa$ B activation.** **A.** Transduction of Hsp60-neutralizing antibody (Hsp60N) into the cytoplasm of HeLa cells. Mitotracker Red (Molecular Probes, USA) and DAPI indicate mitochondria and nuclei, respectively. **B.** The transduced Hsp60N antibody bound to endogenous Hsp60. After antibody transfection, the HeLa cell lysates were subjected to precipitation using Protein-A Sepharose beads. The precipitated proteins were immunoblotted for Hsp60. **C.** IKK and JNK1 activation in response to TNF- $\alpha$  in control IgG or Hsp60N antibody-transfected HeLa cells. The *in vitro* kinase activity (KA) was averaged with the values from two independent experiments, and it is represented as a fold increase of the activity versus the unstimulated and control IgG-transfected cells (lane 1). **D.** TNF- $\alpha$ -induced NF- $\kappa$ B transcriptional activation in antibody-transfected cells (\* $P$ <0.01 versus stimulated IgG-transfected cells). doi:10.1371/journal.pone.0009422.g005

NF- $\kappa$ B activation (see Fig. 6), cytosolic Hsp60 seems likely to direct cell survival in resting cancer cells. Collectively, our results suggest that the selective regulation of MnSOD and Bfl-1/A1 expression by cytosolic Hsp60 sufficiently influences cell survival via suppressing mitochondrial ROS burst.

### Cytosolic Hsp60 protects host cells against stressed conditions

Next, the pro-survival activity of cytosolic Hsp60 was investigated *in vivo*. To do this, transgenic mice expressing Hsp60c were generated (Fig. 9A and 9B). The Hsp60c protein was successfully expressed in various tissues, including liver, spleen, and lung (Fig. 9C). The IKK activation was markedly enhanced in the Hsp60c-expressing transgenic mice compared to the control B6 mice when TNF- $\alpha$  was intravenously injected (Fig. 9D). The result indicates that the cytosolic Hsp60 enhanced the TNF- $\alpha$ -induced IKK activation *in vivo*. We then sought an animal model wherein the IKK/NF- $\kappa$ B-dependent cell survival is involved: the diethylnitrosamine (DEN)-induced hepatocyte death [48]. The apoptotic cell death of hepatocytes was indeed increased after DEN injection in four-week-old male mice (Fig. S3). Therefore, the DEN-induced hepatic cell death was examined in Hsp60c-expressing transgenic mice that had been primed with or without TNF- $\alpha$ . TUNEL staining of the liver tissue sections showed that the hepatic cell death was significantly reduced in Hsp60c-expressing transgenic mice compared to control mice (Fig. 9E and 9F). The data indicate that the cytosolic

Hsp60 prevents the stress-induced cell death *in vivo* by promoting IKK/NF- $\kappa$ B activation.

### Discussion

The present study demonstrates that the cytosolic Hsp60 interacts with the IKK complex and enhances its activation. This signaling action of cytosolic Hsp60 affects the induction of the two NF- $\kappa$ B target genes, Bfl-1/A-1 and MnSOD, and thus cell survival. Since Bfl-1/A-1 functions as a tBid and Bak antagonist [2,4] and MnSOD eliminates the superoxide anion inside mitochondria [49], these two genes are ultimately critical for controlling mitochondrial-derived ROS. Indeed, ablation of cytosolic Hsp60 results in the increase of cellular ROS, which in turn triggers the sustained activation of JNK/p38 via ASK-1 and finally induces the cell death, in response to TNF- $\alpha$ . Given that the mitochondrial ROS are causally linked to various human diseases such as cancer, vascular damage, and a variety of degenerative diseases via the accumulation of cellular damage, this new pro-survival circuitry mediated by cytosolic Hsp60 may be of particular important progression of these diseases.

The transcriptional regulation of select NF- $\kappa$ B target genes by cytosolic Hsp60 is attractive issue but unsolved in the present study. The RNase protection assay and the microarray experiment (~24,000 RefSeq-based probe sequences per array, Illumina expression chip) were failed to demonstrate the broad effect of the cytosolic Hsp60 on expression profile of NF- $\kappa$ B target genes. Instead, the quantitative real-time PCR demonstrated the expres-

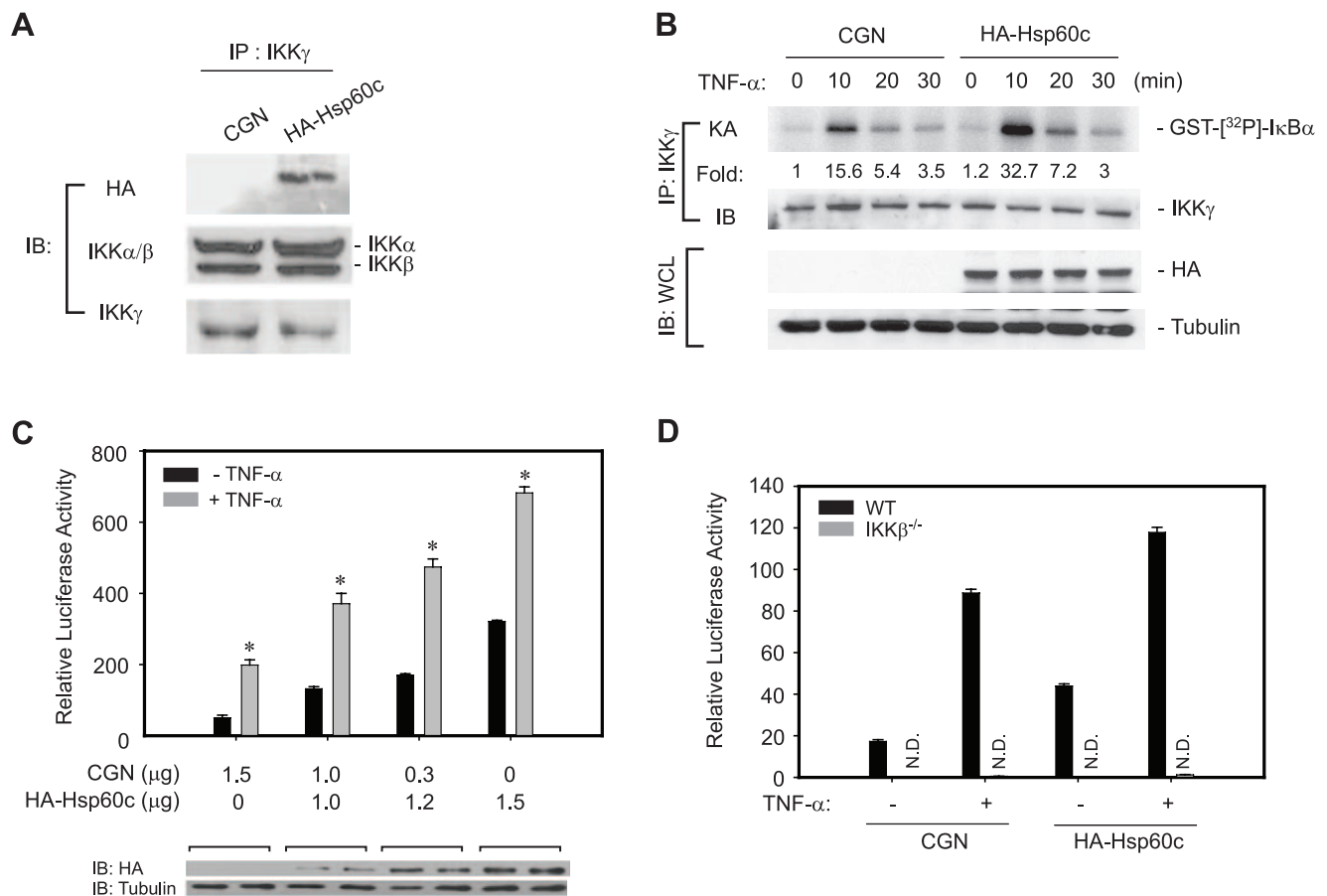


**Figure 6. Cytosol-targeted expression of Hsp60 promotes TNF- $\alpha$ -induced IKK/NF- $\kappa$ B activation.** Cells were transfected with either control (CGN) or Hsp60c-encoding plasmid (HA tag) for 24 hrs and then treated with TNF- $\alpha$ . **A**. Incorporation of ectopically-expressed Hsp60c (HA tag) in IKK complex. **B**. TNF- $\alpha$ -induced IKK activation in HeLa cells. **C** TNF- $\alpha$ -induced NF- $\kappa$ B activation in HeLa cells ( $n=4$ ,  $*P<0.0001$  versus unstimulated counterpart). **D**. TNF- $\alpha$ -induced NF- $\kappa$ B activation in the transfected IKK $\beta$ <sup>-/-</sup> 3T3 cells ( $n=4$ ,  $*P<0.001$  versus stimulated CGN-transfected cells, N.D. not detected).

doi:10.1371/journal.pone.0009422.g006

sional change of the two select target genes, MnSOD and Bfl-1/A1, both of which are known to be related to the mitochondrial function. Although this odd phenomena were hardly investigated in the study, some experimental data can provide a clue. 1) Hsp60 was shown to bind preferentially to IKK $\alpha$  rather than to IKK $\beta$  in the *in vivo* protein binding assay. 2) Direct interaction of Hsp60 and IKK $\alpha$ , but not IKK $\beta$ , in the nucleus was often observed in the immunogold staining. IKK $\alpha$  is known to regulate NF- $\kappa$ B transcriptional activity in the nucleus [31,32] rather than I $\kappa$ B phosphorylation [50]. Supposedly, when the Hsp60-IKK $\alpha$  complex translocate to nucleus, the Hsp60 may directly guide IKK $\alpha$  to the promoter of particular gene set (e.g, MnSOD and Bfl-1/A1). This is similar to the way exemplified in the regulation of select p53 target genes by human cellular apoptosis susceptibility (hCAS) protein [51]. Otherwise, it may be possible that the Hsp60 modulates the ability of IKK $\alpha$  or presumably IKK $\beta$  as well, to phosphorylate the other substrates such as RelA, SMRT, and histone H3 [52], which thus indirectly affects the NF- $\kappa$ B transcription. For example, the IKK $\alpha$ -mediated phosphorylation of SMRT corepressor allows the recruitment of NF- $\kappa$ B to promoters [53], and IKK $\alpha$ -mediated phosphorylation of histone H3 affects the chromatin structure [31,32]. However, our inciting speculation needs an investigation.

On the other hand, the functional significance of Hsp60-IKK $\alpha$  interaction was also investigated in non-canonical NF- $\kappa$ B

signaling, RANK-induced osteoclastogenesis [54]. IKK $\alpha$ -mediated NF- $\kappa$ B pathway is essential for RANK-induced osteoclastogenesis [55,56]. As shown in Fig. S5, the reduction of cytosolic Hsp60 expression using antisense ODN (AS-1) clearly suppressed the RANK-induced osteoclast formation from the bone marrow-derived macrophage/monocytic (BMM) cells, as quantified by TRAP assay. Since TNF- $\alpha$ -induced osteoclast formation [57] was also markedly suppressed, this result indicates that cytosolic Hsp60 can function in the NF- $\kappa$ B activation pathway via interacting with non-canonical as well as canonical IKK complex.

Since Hsp60 is exclusively targeted to mitochondria after translation, the cytosolic Hsp60 is presumed to be of mitochondrial origin. In fact, the mitochondrial release of Hsp60 in staurosporine-treated Jurkat T cells has been shown [29]. We also observed the same result in staurosporine-treated HeLa cells (Fig. S4). Since the Hsp60 protein was detected in the mitochondrial intermembrane space in immunogold EM data, we believe that this pool of Hsp60 protein can be released. This is similar to the case of pro-apoptotic mitochondrial factors. For example, AIF is a mitochondrial inner membrane protein (62-kDa in mature form) and is released after proteolytic shedding to a 57-kDa form upon proapoptotic stimuli [58,59]. HtrA2/Omi (51-kDa serine protease) is released from the mitochondrial intermembrane space [60,61]. In addition, the fact that the antisense-ODN (AS-1) used in the

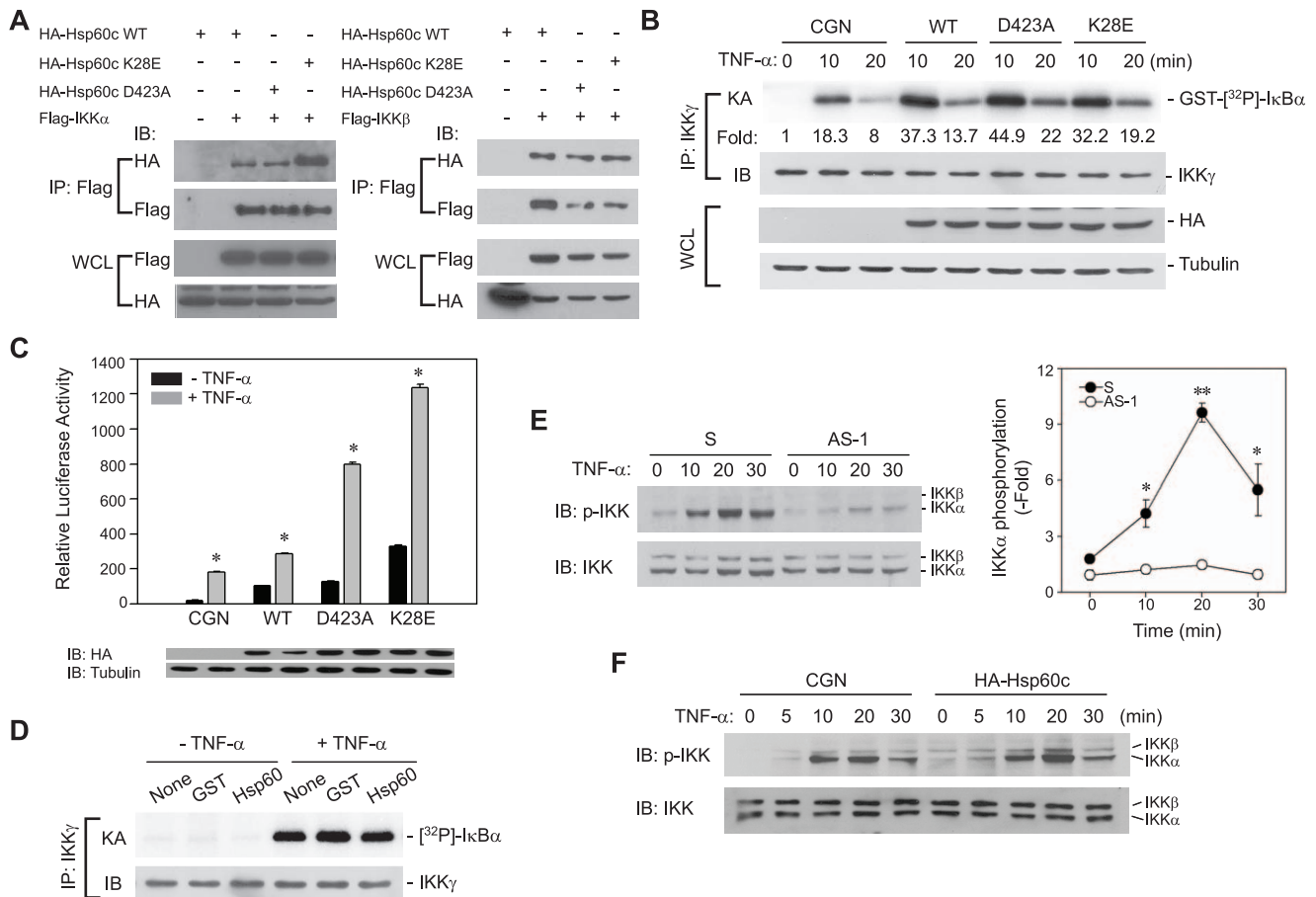


**Figure 7. Cytosolic Hsp60 regulates IKK phosphorylation independently of chaperone activity.** **A.** Association of Hsp60c wild-type (WT) and mutants with IKK $\alpha$  and IKK $\beta$ . The indicated proteins were co-expressed in 293T cells as shown in Fig. 3A. **B** and **C.** IKK (**B**) and NF- $\kappa$ B transcriptional activation (**C**) in cells expressing Hsp60c wild-type and chaperone-inactive mutants. The kinase and reporter activities were analyzed as described in Fig. 4 (for reporter assay,  $n=6$ ,  $*P<0.0001$  versus unstimulated counterpart). **D.** *In vitro* kinase activity of IKK in the presence of recombinant Hsp60 protein. The IKK complex was immunoprecipitated from HeLa cell lysates and incubated with or without the indicated GST proteins (20  $\mu$ g each) in the kinase reaction buffer for 10 min before the kinase reaction. **E.** Serine phosphorylation of IKK $\alpha$ / $\beta$  in HeLa cells transfected with AS-1 ODN. Data in the graph are means  $\pm$  S.D. ( $n=3$ ,  $*P<0.02$ ,  $*P<0.001$ ). **F.** Serine phosphorylation of IKK $\alpha$ / $\beta$  in Hsp60c-expression HeLa cells. A representative blot is shown ( $n=3$ ). doi:10.1371/journal.pone.0009422.g007

study targets MTS-encoding region of Hsp60 mRNA transcript but reduces the level of cytosolic Hsp60 is also supportive.

Hsp60 once located in the cytosol exhibited the faster turnover compared to the mitochondrial one. Its rapid turnover is controlled in a proteasome-dependent manner, but it is unlikely due to the structural instability because the cHsp60 protein lacking MTS sequence was successfully expressed and purified in soluble form. Nonetheless, since we cannot exclude the possibility of natural mitochondrial targeting error, the investigation on how mitochondrial Hsp60 is released and whether the turnover of cytosolic Hsp60 depends on ubiquitination is on-going.

Cytosolic Hsps such as Hsp70 and Hsp90 are known to broadly participate in cell signaling [30]. As a chaperone protein, they stabilize or destabilize the large signaling protein complexes. Since the interaction of Hsp60 and IKK complex was unaffected by TNF- $\alpha$  stimulation, the mode of Hsp60 action was initially thought to be the same. However, our results shown suggest a unique feature of the signaling function of cytosolic Hsp60. Briefly, the polymerization-defective or ATPase-inactive mutant of Hsp60 enhanced IKK/NF- $\kappa$ B activation much more effectively than the wild-type Hsp60 did (see Fig. 8). This suggests that Hsp60 likely functions as a non-

chaperonic monomer rather than a chaperone polymer in augmenting NF- $\kappa$ B activation. Some experimental evidences also favorably support the possibility of non-chaperonic function of cytosolic Hsp60: 1) the introduction of the Hsp60N neutralizing antibody did not affect the amount of IKK core subunits in the lysate and immunoprecipitate, and 2) the AS-ODN did not affect the amount of IKK core subunits in the high-molecular-weight fractions (>600 kDa) from gel filtration chromatography (data not shown). These results indicate that the cytosolic Hsp60 is not involved in the stability of the IKK complex. Rather, our study clearly demonstrates that cytosolic Hsp60 is involved in the regulation of IKK phosphorylation in the activation T-loop. Therefore, the cytosolic Hsp60 may act on either enhancing the interaction of the IKK complex with an upstream kinase or the oligomerization-dependent auto-phosphorylation [52]. In any case, it can be a novel mechanism of the IKK activation in collaboration with the ubiquitin-dependent mechanism.

In summary, cytosolic presence of Hsp60 is frequently detected and play signaling roles in the cell types, e.g. cardiac myocytes and hepatocytes [37,62,63]. And also there are attempts to approach anti-cancer therapy through understanding the presence and

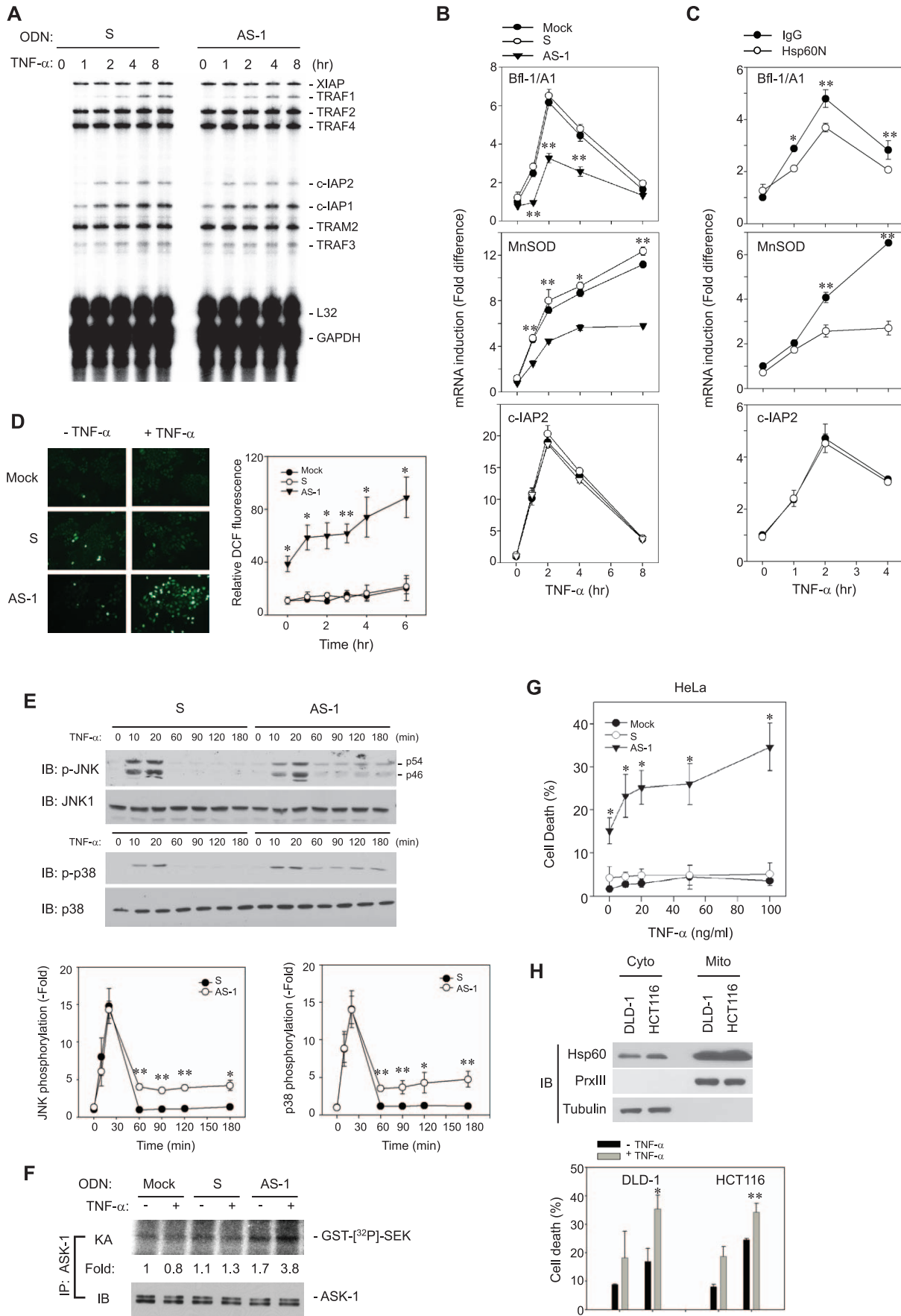


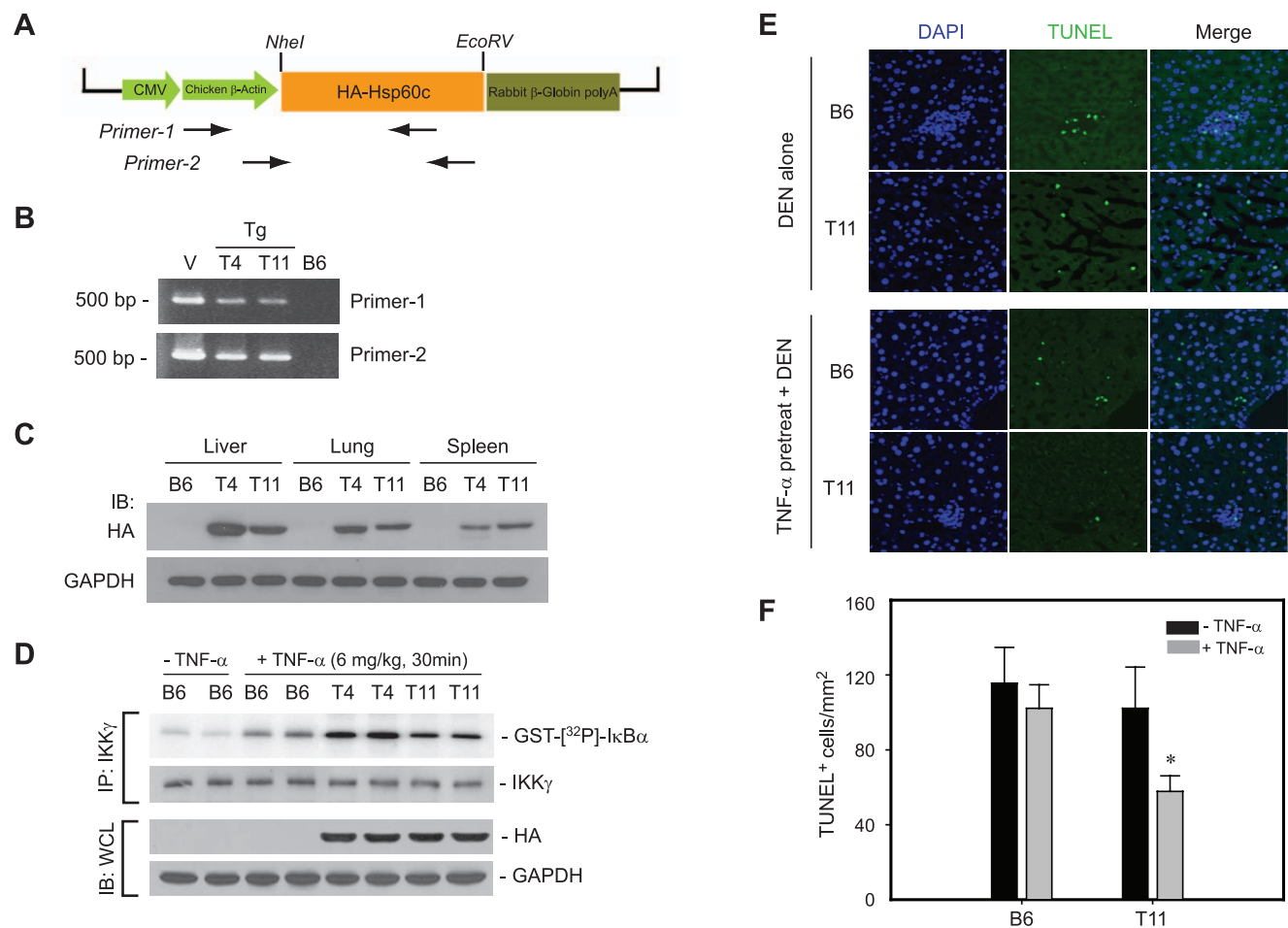
**Figure 8. Loss of cytosolic Hsp60 induces cell death in response to TNF- $\alpha$  by inducing ROS and ASK-1 activation.** **A.** RNase protection assay for induction of anti-apoptotic genes in ODN-transfected cells. The autoradiogram shown is a representative of three independent experiments. **B** and **C.** QPCR for induction of endogenous NF- $\kappa$ B target genes in ODN-transfected cells (**B**) and antibody-transfected cells (**C**) ( $n=3$ ,  $*P<0.01$ ,  $**P<0.001$ ). **D.** TNF- $\alpha$ -mediated production of cellular ROS in ODN-transfected cells. The representative images are shown. Data are means  $\pm$  S.D. of fold increase versus untreated mock cells of the relative DCF fluorescence ( $n=4$ ,  $*P<0.05$ ,  $**P<0.001$ ). **E.** JNK and p38 MAPK activation in ODN-transfected cells. Representative blots are shown. Data in the graphs are means  $\pm$  S.D. of the intensities of phospho-JNK (p46) or phospho-p38 bands that had been normalized by the corresponding non-phospho-bands ( $n=3$ ,  $*P<0.05$ ,  $**P<0.001$ ). **F.** ASK-1 activation in ODN-transfected cells. The kinase activity (KA) was averaged with the values from two independent experiments, and presented as a fold increase of the activity versus the unstimulated and mock-transfected cells (lane 1). **G.** TNF- $\alpha$ -induced cell death in mock or ODN-transfected HeLa. Data are means  $\pm$  S.D. ( $n=3$ ,  $*P<0.01$ ). **H.** TNF- $\alpha$ -induced cell death of colon carcinoma cells transfected with ODNs. The level of Hsp60 in subcellular fractions is shown (*Upper*). Data in the graph are means  $\pm$  S.D. ( $n=3$ ,  $*P<0.05$ ,  $**P<0.01$ ). Cell death was analyzed by FACS after staining with annexin V-fluorescein isothiocyanate and propidium iodide. doi:10.1371/journal.pone.0009422.g008

function of Hsp60 proteins in the extra-mitochondrial compartments [25]. Our study demonstrates for the first time that, by directly interacting and regulating IKK activation, the cytosolic Hsp60 serves as survival guidance controlling mitochondrial-derived ROS through NF- $\kappa$ B target gene expression. Therefore, either antagonizing the interaction of Hsp60 with IKK or reducing the level of the cytosolic Hsp60 could be an additional therapeutic tool in anti-inflammatory strategy.

## Materials and Methods

### Reagents

Antibodies to IKK $\alpha$  (B-8), IKK $\gamma$  (FL-419), Hsp90 (H-114), Hsp60 (K-19 and N-20), I $\kappa$ B $\alpha$  (C-21), JNK1 (C-17), ASK-1 (H-300 and F-9), glutathione S-transferase (B14), and goat IgG were purchased from Santa Cruz Biotechnology (Santa Cruz, US); Anti-Flag antibody (M2) was purchased from Sigma; Anti-hexahistidine



antibody was obtained from Qiagen; Antibodies to phosphor-IKK, IKK $\alpha$ , and IKK $\beta$  were from Cell Signaling Technology; Normal mouse and rabbit IgG were from Amersham Bioscience; Anti-cytochrome c antibody were from BD Pharmingen; Antibodies to Peroxiredoxin III (Prx III), MnSOD (2AI), Hemagglutinin epitope (HA), and GAPDH were provided by AbFrontier (Seoul, Korea); Recombinant human TNF- $\alpha$  was purchased from Invitrogen (Grand Island, USA). The phosphorothioate oligodeoxynucleotides (ODNs), including the antisense and sense sequences, were synthesized by Hokkaido System Sciences Co. (Hokkaido, Japan). The full-length human I $\kappa$ B protein was a kind gift of W. Jeong (Ewha Womans University, Korea) [64].

### Plasmids

The full-length cDNA of human Hsp60 was obtained from the National Genome Information Center (Daejeon, Korea). A truncated form of Hsp60, designated as Hsp60c, which lacks a mitochondrial targeting sequence (MTS; amino acids 1–26 based on human sequence), was amplified by PCR and subcloned into the pCGN-HA (a kind gift of Dr. W. Herr, Cold Spring Harbor Laboratory) and pGEX-4T1 (Amersham) vectors, by which the HA-tagged and GST-fused Hsp60c expression plasmids, respectively, were constructed.

CRE-, NF-AT-, and AP1-dependent (pAP1<sub>7x</sub>-Luc) firefly luciferase reporters were obtained from Stratagene. Luciferase reporter plasmids harboring the IFN $\beta$ -derived NF- $\kappa$ B enhancer sequences [65] was a kind gift of S. Y. Lee (Ewha Womans University, Korea). Human IKK  $\alpha$ ,  $\beta$ , and  $\gamma$  cDNAs [66,67] were subcloned into the pCMV2-FLAG or baculovirus expression vector pFastBac-HTa (Invitrogen). The pFastBac constructs, encoding each of IKK $\alpha$ ,  $\beta$ , and  $\gamma$ , were used for production of high-titer recombinant baculovirus stocks ( $\sim 1 \times 10^7$  pfu/ml), according to the manufacturer's protocol. The pPuro plasmids encoding human Bcl-2 or Bcl-X<sub>L</sub> were kindly provided by D.Y. Shin (Dankook University, Korea) [68]. The plasmid pGEX-4T1-SEK1 (K129R) [69] was used for production of GST-SEK1(K129R) recombinant protein. Site-directed mutagenesis was performed using a QuikChange mutagenesis kit (Stratagene).

### Immuno-affinity purification of IKK complex and ESI-q-TOF tandem mass spectrometry

HeLa S3 cells (20 ml packing volume from 20-l suspension culture) were gently lysed in 200 ml of lysis buffer A (20 mM HEPES (pH 7.5), 150 mM NaCl, 1 mM EDTA, 2 mM EGTA, 1% Triton X-100, 10% glycerol, 1 mM AEBSEF, 1 mM Na<sub>3</sub>VO<sub>4</sub>, 5 mM NaF, 10  $\mu$ g/ml aprotinin and leupeptin). The lysate (2 grams of total protein) was precleared with agarose beads alone for 1 hr, and then incubated overnight with anti-IKK $\alpha$ -conjugated agarose beads (2 mg/ml IgG, Santa Cruz Biotechnology). After extensively washing four times with the lysis buffer, the beads were loaded onto a column and rinsed twice with phosphate-buffered saline. The precipitated proteins were eluted twice with 1 ml of 0.1 M glycine buffer (pH 2.5). The protein eluates were immediately neutralized by adding 1 M Tris HCl buffer (pH 8.0) and separated on a 10% denaturing gel. The gel was subsequently stained with silver nitrate, and the silver-stained spots were subjected to in-gel trypsin digestion with minor modifications as follows. Briefly, the gel spots were excised with a scalpel and destained by washing with 15 mM K<sub>4</sub>Fe(CN)<sub>6</sub>, 50 mM sodium thiosulfate. The gel pieces were crushed, dehydrated by adding acetonitrile, rehydrated by adding 10–20  $\mu$ l of 25 mM ammonium bicarbonate with 10 ng/ $\mu$ l of sequencing grade trypsin (Promega), and incubated at 37°C for 15–17 h. The peptides in the supernatant were transferred to a new tube and extracted twice

by adding 50  $\mu$ l of a solution containing 60% acetonitrile and 0.1% trifluoroacetic acid. The extracted solutions were pooled and evaporated to dryness in a SpeedVac vacuum centrifuge. The tandem mass spectral (MS/MS) analysis for peptide sequencing was done with nano flow reversed-phased HPLC/ESI/MS with a mass spectrometer (Q-TOF Ultima<sup>TM</sup> global, Waters Co. UK). Peptides were separated by using a C<sub>18</sub> reversed-phase 75 $\mu$ m i. d.  $\times$  150 mm analytical column (3  $\mu$ m particle size, Atlantis<sup>TM</sup> dC18, Waters) with an integrated electrospray ionization Silica-Tip<sup>TM</sup> ( $\pm 10$   $\mu$ m, New Objective, USA). In detail, 5  $\mu$ l of peptide mixtures were dissolved in buffer A (water/ACN/formic acid; 95:5:0.2, v/v), injected onto a column and eluted by a linear gradient of 5–80% buffer B (water/ACN/formic acid; 5:95:0.2, v/v) over 120 min. Samples were desalted on a line prior to separation using a trap column (i.d. 0.35  $\times$  50 mm, OPTI-PAK<sup>TM</sup> C<sub>18</sub>, Waters) cartridge. Initially, the flow rate was set to 200 nL/min by a split/splitless inlet and the capillary voltage (3.0 keV) was applied to the HPLC mobile phase before spraying. Chromatography was performed online using the instrument's control software MassLinx of Q-TOF Ultima<sup>TM</sup> global. The mass spectrometer was programmed to record scan cycles composed of one MS scan followed by MS/MS scans of the eight most abundant ions in each MS scan. MS parameters for efficient data-dependent acquisition were intensity ( $>10$ ) and number of components (3–4) to be switched from an MS to MS/MS analysis. Following positive identification, all identified peptides from database search (Mascot) were excluded in the next run analysis until full sequence coverage was obtained. Database analyses using the database search programs including Mascot (global search engine), Proteinlynx 2.1 (Waters Co., UK) and MODi (Korea, <http://modi.uos.ac.kr/modi/>), provided almost full sequence coverage on selective exclusion monitoring. MS/MS spectra were matched against amino acid sequences in SwissProt. Precursor ion mass corrections and a fragment ion mass tolerance of 0.2 Da were used to consider as 2 missed cleavages.

### Immunolectron microscopy

The HeLa cells ( $1 \times 10^7$  cells) were harvested and fixed for 1 hr, at room temperature in 0.1 M cacodylate buffer (pH 7.2) that contained 0.5% glutaraldehyde. After rinsing with cold distilled water, they were dehydrated through an ethanol treatment series at 4°C. They were infiltrated with LR White resin (London Resin, Berkshire, England) at 4°C and embedded in LR White resin in a gelatin capsules (Nisshin EM, Tokyo, Japan). Polymerization of the resin was carried out at 50°C for 24 hrs. Serial sections (120–200 sections per one sample), 70 nm in thickness, were attached to formvar-coated nickel grids. Sections were incubated in 50mM glycine for 5 min at room temperature. After rinsing with PBS, sections were incubated in 3% BSA for 30 mins at room temperature. Then, they were incubated with primary antibodies (goat anti-human Hsp60 (SC-1722), mouse anti-human IKK $\alpha$  (SC-7606), mouse anti-IKK $\beta$  (SC-8014), diluted 1:100 in PBS) for 2 hrs, at room temperature. After washing five times with Tween-PBS (PBS plus 0.5% Tween-20), sections were treated with 20 nm- and 40 nm-diameter colloidal gold conjugated to anti-goat and anti-mouse IgG + IgM antibodies, respectively (BB International, UK, diluted 1:20 in PBS) for 2 hrs, at room temperature. The sections were washed three times with Tween-PBS and then washed three times with distilled water. Sections were stained with 4% uranyl acetate for 5 mins and with lead citrate for 5 min. To examine the specificity of the primary antibody, a treatment of sections was performed with the same procedure without of the primary antibody. For double staining, antibody reactions were repeated with the second set of primary and secondary antibodies.

Finally, samples were observed with a Tecnai G2 Spirit Twin transmission electron microscope (FEI Co., USA) and a JEM ARM 1300S high-voltage electron microscope (JEOL, Japan).

### Subcellular fractionation

The subcellular fractions for immunoprecipitation were acquired by differential centrifugation. Briefly, the HeLa cells ( $2 \times 10^7$  cells) were harvested, rinsed twice with ice-cold PBS, and resuspended in 1 ml of a homogenization buffer (20 mM HEPES (pH 7.5), 0.5 mM EDTA, 0.5 mM EGTA, 2 mM  $MgCl_2$ , 25 mM KCl, 1 mM AEBBSF, 1 mM  $Na_3VO_4$ , 5 mM NaF, 5  $\mu$ g/ml aprotinin, and 5  $\mu$ g/ml leupeptin) containing 0.25 M sucrose. After rupturing the cells using a glass Dounce homogenizer, the post-nuclear supernatants were obtained from the homogenate by centrifugation at 750 *g* for 10 min. The supernatants were separated into pellets (mitochondrial fraction) and supernatants (cytosol fraction) by centrifugation at 15,000 *g* for 15 min. For ODN transfected cells, the subcellular fractions were obtained using the ProteoExtract subcellular proteome extraction kit (Roche). The purity of each fraction was verified by selective markers:  $\alpha$ -tubulin as a cytosolic marker, inner membrane protein cytochrome c oxidase 4 (COX4) and matrix protein peroxiredoxin III (Prx III) [70] as mitochondrial markers. For best comparison, the mitochondrial fraction was loaded at a volume of one-fifth of the corresponding cytosolic fraction.

### *In vitro* binding assay with recombinant proteins

The Sf9 insect cells were infected with each of recombinant baculovirus stocks harboring IKK $\alpha$ -, IKK $\beta$ -, and IKK $\gamma$ - encoding bacmids. The insect lysates expressing (His)<sub>6</sub>-tagged IKKs were incubated with 1.0  $\mu$ g of GST-Hsp60 proteins pre-bound to glutathione-Spharose beads (Amersham Pharmacia Biotech) at 4°C for 2 hrs. The beads were washed again three times with a cold lysis buffer A. The proteins bound to the beads were eluted by boiling in a SDS sample buffer and then subjected to immunoblot analyses as indicated in Fig. 1c.

### Transfection

The ODNs (200 nM, unless indicated) was transfected for 24 hrs using Oligofectamine™ reagent (Invitrogen, USA). The plasmid transfection was achieved using Fugene-6 reagent (Roche, USA). The antibody was transduced using a Chariot™ protein delivery kit (Active Motif Co., USA), according to the manufacturer's instruction.

### Immunoprecipitation and *in vitro* kinase assay

The HeLa cells were treated with or without TNF- $\alpha$  (10 ng/ml) for the indicated time periods, rinsed once with cold PBS, and lysed in the lysis buffer A. The cell lysates were precleared with 10  $\mu$ l of protein A/G agarose beads (Amersham Biosciences) for 1 hr. The cleared lysates were incubated with 2  $\mu$ g of Hsp60, IKK $\alpha$ , IKK $\beta$ , or IKK $\gamma$  antibodies for 3 hrs and mixed with 20  $\mu$ l of protein A/G agarose beads. The lysates were further rotated overnight at 4°C. The beads were washed three times with 1 ml of lysis buffer A. The final protein precipitates were subjected to immunoblot analyses. The immune complexes were visualized by using an enhanced chemiluminescence kit (Amersham Biosciences, USA).

For the *in vitro* kinase assay, the IKK, JNK1 or ASK-1 was immunoprecipitated with anti-IKK $\gamma$  (FL-419) or anti-JNK1 (C-17) or anti-ASK-1 (H-300) antibody, respectively. The beads containing the IKK complex or JNK1 were washed twice with lysis buffer and further twice with a kinase buffer (20 mM HEPES, pH 7.4, 5 mM  $MgCl_2$ , 10 mM  $\beta$ -glycerolphosphate, 1 mM  $Na_3VO_4$ ,

2 mM NaF, and 1 mM dithiothreitol), and then incubated in 40  $\mu$ l of a kinase buffer containing 10  $\mu$ M ATP, 0.6  $\mu$ Ci [ $\gamma$ -<sup>32</sup>P] ATP, and 2  $\mu$ g of either GST-IkB (1–54) or GST-c-Jun or GST-SEK1 (K129R) at 30°C for 30 min. The reaction was stopped by adding 20  $\mu$ l of 3 $\times$ SDS sample buffer. After boiling, the half of reaction mixture was resolved on a 10% denaturing gel and the radioactivity was detected by autoradiography. The other half of reaction mixture was used for immunoblotting of the immunoprecipitated kinase proteins (note: anti-ASK-1 antibody (F-9) for detecting ASK-1).

### Measurement of Intracellular ROS

Intracellular ROS generation was assessed with an oxidation sensitive fluoresce dye, 5,6-chloromethyl-2', 7'-dichlorodihydrofluorescein diacetate (CM-H<sub>2</sub>DCFDA, Molecular Probes, USA) as described [71]. The HeLa cells ( $3 \times 10^5$ ) were plated on 35-mm dishes and transfected with ODNs for 24 hrs. The cells were then deprived of serum for 6 hrs and stimulated with TNF- $\alpha$  in phenol red-free media for the indicated periods of time. After stimulation, the cells were quickly rinsed with Krebs-Ringer solution and incubated for 5 min with 5  $\mu$ M CM-H<sub>2</sub>DCFDA. The DCF fluorescence was collected for 10 seconds with an inverted Axiovert200 fluorescence microscope (Zeiss). The relative DCF fluorescence was obtained by averaging the fluorescence intensities of the 60–80 cells in each image using ImageQuant™ software (GE Healthcare). Note that the detached round cells were omitted from quantification.

### RNase protection assay

ODN-pretreated HeLa cells were treated with or without TNF- $\alpha$  (10 ng/ml) for the indicated times. The total RNA was extracted with Trizol (Invitrogen). The ribonuclease (RNase) protection assay was performed according to the manufacturer's protocol (BD PharMingen). Briefly, the human apoptosis template set hAPO-5 was labeled with [ $\alpha$ -<sup>32</sup>P]-uridine triphosphate. The RNA (10  $\mu$ g) and  $6 \times 10^5$  cpm of the labeled probes were subjected to hybridization. After the RNase treatments, the protected probes were resolved on 5% urea-polyacrylamide gel and detected by autoradiography.

### Quantitative PCR (qPCR)

Total RNA was extracted using Trizol reagent (Invitrogen) from the HeLa cells stimulated with TNF- $\alpha$  for indicated periods of time. RNA (1.5  $\mu$ g) was reverse transcribed using ImProm-II RT system (Promega). The real-time PCR was performed using specific primers in the presence of SYBR Green (Applied Biosystems) inside a fluorescent temperature cycler (ABI Prism 7000 sequence detection system, Applied Biosystems). The fluorescence signals were quantified by a comparative cycle threshold method. The actin mRNA was used for an endogenous control.

### Transgenic mice generation

The HA-tagged human Hsp60c lacking mitochondrial signal sequence was PCR-amplified and subcloned into pCAGGS transgenic (Tg) vector, which contains the chicken  $\beta$ -actin promoter, using *NheI* and *EcoRV* sites. The HA-Hsp60c Tg construct was linearized by digestion with *SalI* and *PstI* and then microinjected into eggs from C57BL/6j females. The transgenic founders were genotyped as described below. Two of the six positive transgenic lines, designated T4 and T11, were chosen for this study. The tail DNA was used for genotyping. In brief, mouse tails were incubated overnight in 100 mM Tris, pH 8.0, 0.5 mM

EDTA, 200 mM NaCl, 0.2% SDS, and 100 µg of proteinase K at 55°C. DNA was extracted with phenol:chloroform:isoamyl alcohol (25:24:1) and precipitated with isopropanol. Genomic PCR was performed by using two primer sets (set 1: forward primer, 5'-ATGGCTTCTAGCTATCCTTATG-3', and reverse primer, 5'-GTAGCAACCTGTGCAATTTCTTC-3'; set 2: forward primer, 5'-CTGCTAACCATGTTTCATGCC-3' and reverse primer, 5'-ACAAGTTTCTAGCTCCAATGTTTTTGTA-3'). All the experiments were performed with 4-week-old males.

### Analysis of apoptotic cells in DEN-induced liver damage

The four-week-old male mice were injected intravenously with phosphate-buffered saline (PBS, pH 7.4) or TNF- $\alpha$  (6 µg/kg) via the lateral tail vein 6 hrs before intraperitoneal administration of DEN (10 mg/kg). After 48 hrs of DEN treatment, animals were sacrificed and rapidly perfused with PBS followed by 4% paraformaldehyde. The livers were removed and frozen in OCT embedding medium, and then a series of tissue sections (10 µm in thickness) was obtained in cryostat (Leica). The sections were incubated in 50 µl of terminal deoxynucleotidyl transferase-mediate uridine 5'-triphosphate-biotin nick-end labeling (TUNEL) fluorescent reaction mixture (In situ Cell Death Detection Kit, Roche Diagnostics) for 60 mins at 37°C in a dark chamber, washed and subsequently counterstained with 4',6'-diamidino-2-phenylindole (DAPI, 1 µg/ml, Sigma) for 30 mins. The sections were mounted using the Vectashield mounting medium and examined using a LSM510 confocal laser-scanning microscope (Carl Zeiss, Germany). TUNEL-positive cells were counted and averaged from three tissue sections per mouse. All animal experiments were performed in compliance with the institutional guidelines (Ewha Womans University, Korea) for the care and use of laboratory animals.

### In vitro osteoclastogenesis

The non-adherent bone marrow-derived monocytes/macrophages (BMM) lineage cells derived from C57BL/6 mice were seeded and cultured in  $\alpha$ -MEM (Invitrogen) containing 10% FBS and M-CSF (10 ng/ml, R&D systems). After 2 days, the nonadherent cells including lymphocytes were removed and the adherent cells were used as BMMs. The differentiation of BMM to osteoclast cells was induced by treating them with either soluble RANKL (50 ng/ml, Peprotech) or TNF- $\alpha$  (20 ng/ml) in the presence of M-CSF. After 5 days of induction, the cells were fixed and stained for tartrate-resistant acid phosphatase (TRAP). The cells were observed using a Zeiss Axiovert 200 microscope (Carl Zeiss) equipped with a plan-Neofluor objective lens. The images were analyzed using AxioVision 3.1 software (Carl Zeiss). The TRAP-positive multinucleated (>3 nuclei) cells were counted as osteoclast-like cells.

### Statistics

Data were analyzed using Student's *t*-test on SigmaPlot 8.0 software. The *P* values were derived to assess statistical significance and indicated on figure panels.

### Supporting Information

**Figure S1** Action of Hsp60-specific antisense oligodeoxynucleotide (AS-ODN). A. Schematic representation of two different Hsp60 AS-ODNs. B. Hsp60 expression in mock- or ODN-transfected HeLa cells. C. TNF- $\alpha$ -induced MAP kinase activation in HeLa cells transfected with either mock or ODNs. The activation was analyzed by using phospho-specific antibodies. The phosphoblots were re-probed with whole protein antibodies for equal loading. D. Activation of various transcription factors in mock- or ODN-transfected HeLa cells. AP-1 and NF-AT

transcriptional activation were induced by epidermal growth factor (EGF, 100 ng/ml). CRE transcriptional activation was induced by forskolin (1 µM). E. TNF- $\alpha$ -induced NF- $\kappa$ B transcriptional activation in 293T and A549 cells transfected with either mock or ODNs as indicated. In D and E, the relative luciferase activity was measured using an enhanced luciferase assay kit (Promega) and normalized to the  $\beta$ -galactosidase activity. Data are means  $\pm$  S.D. of four independent experiments (In E, \**P*<0.001 and \*\**P*<0.05 versus stimulated S-ODN-transfected cells).

Found at: doi:10.1371/journal.pone.0009422.s001 (2.28 MB EPS)

**Figure S2** Selective role of cytosolic Hsp60 (Hsp60c) in IKK/NF- $\kappa$ B signaling. A. TNF- $\alpha$ -induced JNK activation in HeLa cells expressing Hsp60c (HA tag). B - D. Activation of various transcription factors in HeLa cells transfected with either control vector or Hsp60c (HA tag). AP-1 (B) and NF-AT (C) transcriptional activation were induced by epidermal growth factor (EGF, 100 ng/ml). CRE transcriptional activation (D) was induced by forskolin (1 µM). The relative luciferase activity was measured using an enhanced luciferase assay kit (Promega) and normalized to the  $\beta$ -galactosidase activity. Data are means  $\pm$  S.D. of three independent experiments.

Found at: doi:10.1371/journal.pone.0009422.s002 (1.35 MB EPS)

**Figure S3** DEN induces hepatic cell apoptosis. The four-week-old C57BL/6j male mice were intraperitoneally injected with DEN (10 mg/kg). After the indicated time periods of DEN treatment, animals were sacrificed and processed to prepare tissue sections and images as described in Experimental Procedures. TUNEL positive cells were counted in three tissue sections per mouse. Representative images (A) are shown. Data in the quantitative graph (B) are mean  $\pm$  S.D. of TUNEL positive cells per unit area.

Found at: doi:10.1371/journal.pone.0009422.s003 (4.30 MB EPS)

**Figure S4** Mitochondrial release of Hsp60 in staurosporine-treated HeLa cells. HeLa cells were treated with 1 µM staurosporine and then subjected to subcellular fractionation using the ProteoExtract subcellular proteome extraction kit (Roche). Peroxiredoxin-III (Prx III) and  $\alpha$ -tubulin were used as mitochondrial and cytosolic markers, respectively. In particular, an antioxidant enzyme called Prx III (25-kDa in molecular size), which is present in the mitochondrial matrix, was useful for monitoring mitochondrial rupture. In western blots, the mitochondrial fractions were loaded at the volume of one-fifth of cytosolic fraction for appropriate comparison.

Found at: doi:10.1371/journal.pone.0009422.s004 (1.31 MB EPS)

**Figure S5** Cytosolic Hsp60 plays a significant survival role in RANK-mediated osteoclastogenesis. The ODN-pretreated BMM cells were treated with either RANKL (A) or TNF- $\alpha$  (B) for 5 days in the presence of M-CSF. The TRAP-positive multinucleated osteoclast cells were counted as described in the Experimental Procedures. Data represent the means  $\pm$  SD of triplicate from one of two independent sets of experiments, all of which showed similar results (\* *P*<0.02 versus the stimulated sense-ODN). Representative pictures are shown.

Found at: doi:10.1371/journal.pone.0009422.s005 (7.72 MB EPS)

### Acknowledgments

We are grateful to M. Karin for providing IKK $\alpha$ / $\beta$ <sup>-/-</sup> 3T3 cells, F. Mercurio for sharing Flag-IKK $\alpha$ / $\beta$ -encoding plasmids, and W. Herr for sharing pCGN plasmid vector. We are also grateful to M. S. Lee, T. S. Chang, and G. T. Oh for helping us with IKK 3T3 cell lines, ASK1 assay, and transgenic mice generation, respectively. Finally, we extend our gratitude to members in core research facilities for laboratory animals and mass spectrometry for technical assistance.

## Author Contributions

Conceived and designed the experiments: JNC BC SHL HSK SWK. Performed the experiments: JNC BC KWL DJL DHK JYL ISS HIK SHL

## References

- Karin M, Cao Y, Greten FR, Li ZW (2002) NF-kappaB in cancer: from innocent bystander to major culprit. *Nat Rev Cancer* 2: 301–310.
- Simmons MJ, Fan G, Zong WX, Degenhardt K, White E, et al. (2008) Bfl-1/A1 functions, similar to Mcl-1, as a selective tBid and Bak antagonist. *Oncogene* 27: 1421–1428.
- Bubici C, Papa S, Dean K, Franzoso G (2006) Mutual cross-talk between reactive oxygen species and nuclear factor-kappa B: molecular basis and biological significance. *Oncogene* 25: 6731–6748.
- Wang CY, Guttridge DC, Mayo MW, Baldwin AS, Jr. (1999) NF-kappaB induces expression of the Bcl-2 homologue A1/Bcl-1 to preferentially suppress chemotherapy-induced apoptosis. *Mol Cell Biol* 19: 5923–5929.
- Karin M, Ben-Neriah Y (2000) Phosphorylation meets ubiquitination: the control of NF-[kappa]B activity. *Annu Rev Immunol* 18: 621–663.
- Hayden MS, Ghosh S (2004) Signaling to NF-kappaB. *Genes Dev* 18: 2195–2224.
- Delhase M, Hayakawa M, Chen Y, Karin M (1999) Positive and negative regulation of IkappaB kinase activity through IKKbeta subunit phosphorylation. *Science* 284: 309–313.
- Woronicz JD, Gao X, Cao Z, Rothe M, Goeddel DV (1997) IkappaB kinase-beta: NF-kappaB activation and complex formation with IkappaB kinase-alpha and NIK. *Science* 278: 866–869.
- Malinin NL, Boldin MP, Kovalenko AV, Wallach D (1997) MAP3K-related kinase involved in NF-kappaB induction by TNF, CD95 and IL-1. *Nature* 385: 540–544.
- Lee FS, Peters RT, Dang LC, Maniatis T (1998) MEKK1 activates both IkappaB kinase alpha and IkappaB kinase beta. *Proc Natl Acad Sci U S A* 95: 9319–9324.
- Zhao Q, Lee FS (1999) Mitogen-activated protein kinase/ERK kinase 2 and 3 activate nuclear factor-kappaB through IkappaB kinase-alpha and IkappaB kinase-beta. *J Biol Chem* 274: 8355–8358.
- Yang J, Lin Y, Guo Z, Cheng J, Huang J, et al. (2001) The essential role of MEKK3 in TNF-induced NF-kappaB activation. *Nat Immunol* 2: 620–624.
- Hu MC, Wang Y, Qiu WR, Mikhail A, Meyer CF, et al. (1999) Hematopoietic progenitor kinase-1 (HPK1) stress response signaling pathway activates IkappaB kinases (IKK-alpha/beta) and IKK-beta is a developmentally regulated protein kinase. *Oncogene* 18: 5514–5524.
- Hehner SP, Hofmann TG, Ushmorov A, Dienz O, Wing-Lan Leung I, et al. (2000) Mixed-lineage kinase 3 delivers CD3/CD28-derived signals into the IkappaB kinase complex. *Mol Cell Biol* 20: 2556–2568.
- Wang C, Deng L, Hong M, Akkaraju GR, Inoue J, et al. (2001) TAK1 is a ubiquitin-dependent kinase of MKK and IKK. *Nature* 412: 346–351.
- Heyninck K, Beyaert R (2005) A20 inhibits NF-kappaB activation by dual ubiquitin-editing functions. *Trends Biochem Sci* 30: 1–4.
- Wu CJ, Conze DB, Li T, Srinivasula SM, Ashwell JD (2006) NEMO is a sensor of Lys 63-linked polyubiquitination and functions in NF-kappaB activation. *Nat Cell Biol* 8: 398–406.
- Zhou H, Wertz I, O'Rourke K, Ultsch M, Seshagiri S, et al. (2004) Bcl10 activates the NF-kappaB pathway through ubiquitination of NEMO. *Nature* 427: 167–171.
- Broemer M, Krappmann D, Scheidereit C (2004) Requirement of Hsp90 activity for IkappaB kinase (IKK) biosynthesis and for constitutive and inducible IKK and NF-kappaB activation. *Oncogene* 23: 5378–5386.
- Chen G, Cao P, Goeddel DV (2002) TNF-induced recruitment and activation of the IKK complex require Cdc37 and Hsp90. *Mol Cell* 9: 401–410.
- Park KJ, Gaynor RB, Kwak YT (2003) Heat shock protein 27 association with the I kappa B kinase complex regulates tumor necrosis factor alpha-induced NF-kappa B activation. *J Biol Chem* 278: 35272–35278.
- Ran R, Lu A, Zhang L, Tang Y, Zhu H, et al. (2004) Hsp70 promotes TNF-mediated apoptosis by binding IKK gamma and impairing NF-kappa B survival signaling. *Genes Dev* 18: 1466–1481.
- Prajapati S, Verma U, Yamamoto Y, Kwak YT, Gaynor RB (2004) Protein phosphatase 2Cbeta association with the IkappaB kinase complex is involved in regulating NF-kappaB activity. *J Biol Chem* 279: 1739–1746.
- Ducut Sigala JL, Bottero V, Young DB, Shevchenko A, Mercurio F, et al. (2004) Activation of transcription factor NF-kappaB requires ELKS, an IkappaB kinase regulatory subunit. *Science* 304: 1963–1967.
- Cappello F, de Macario EC, Marasa L, Zummo G, Macario AJ (2008) Hsp60 expression, new locations, functions, and perspectives for cancer diagnosis and therapy. *Cancer Biol Ther* 7.
- Calderwood SK, Mambula SS, Gray PJ, Jr. (2007) Extracellular heat shock proteins in cell signaling and immunity. *Ann N Y Acad Sci* 1113: 28–39.
- Kirchhoff SR, Gupta S, Knowlton AA (2002) Cytosolic heat shock protein 60, apoptosis, and myocardial injury. *Circulation* 105: 2899–2904.
- Xanthoudakis S, Roy S, Rasper D, Hennessey T, Aubin Y, et al. (1999) Hsp60 accelerates the maturation of pro-caspase-3 by upstream activator proteases during apoptosis. *Embo J* 18: 2049–2056.
- Samali A, Cai J, Zhivotovsky B, Jones DP, Orrenius S (1999) Presence of a pre-apoptotic complex of pro-caspase-3, Hsp60 and Hsp10 in the mitochondrial fraction of jurkat cells. *Embo J* 18: 2040–2048.
- Beere HM (2005) Death versus survival: functional interaction between the apoptotic and stress-inducible heat shock protein pathways. *J Clin Invest* 115: 2633–2639.
- Anest V, Hanson JL, Cogswell PC, Steinbrecher KA, Strahl BD, et al. (2003) A nucleosomal function for IkappaB kinase-alpha in NF-kappaB-dependent gene expression. *Nature* 423: 659–663.
- Yamamoto Y, Verma UN, Prajapati S, Kwak YT, Gaynor RB (2003) Histone H3 phosphorylation by IKK-alpha is critical for cytokine-induced gene expression. *Nature* 423: 655–659.
- Cogswell PC, Kashatus DF, Keifer JA, Guttridge DC, Reuther JY, et al. (2003) NF-kappa B and I kappa B alpha are found in the mitochondria. Evidence for regulation of mitochondrial gene expression by NF-kappa B. *J Biol Chem* 278: 2963–2968.
- Bozner P, Wilson GL, Druzhyna NM, Bryant-Thomas TK, LeDoux SP, et al. (2002) Deficiency of chaperonin 60 in Down's syndrome. *J Alzheimers Dis* 4: 479–486.
- Briones P, Vilaseca MA, Ribes A, Vernet A, Lluich M, et al. (1997) A new case of multiple mitochondrial enzyme deficiencies with decreased amount of heat shock protein 60. *J Inher Metab Dis* 20: 569–577.
- Huckriede A, Heikema A, Sjollemma K, Briones P, Agsteribbe E (1995) Morphology of the mitochondria in heat shock protein 60 deficient fibroblasts from mitochondrial myopathy patients. Effects of stress conditions. *Virchows Arch* 427: 159–165.
- Park SG, Lee SM, Jung G (2003) Antisense oligodeoxynucleotides targeted against molecular chaperonin Hsp60 block human hepatitis B virus replication. *J Biol Chem* 278: 39851–39857.
- Steinhoff U, Zugel U, Wand-Wurtenberger A, Hengel H, Rosch R, et al. (1994) Prevention of autoimmune lysis by T cells with specificity for a heat shock protein by antisense oligonucleotide treatment. *Proc Natl Acad Sci U S A* 91: 5085–5088.
- Morris MC, Depollier J, Mery J, Heitz F, Divita G (2001) A peptide carrier for the delivery of biologically active proteins into mammalian cells. *Nat Biotechnol* 19: 1173–1176.
- Horovitz A, Bochkareva ES, Girshovich AS (1993) The N terminus of the molecular chaperonin GroEL is a crucial structural element for its assembly. *J Biol Chem* 268: 9957–9959.
- White ZW, Fisher KE, Eisenstein E (1995) A monomeric variant of GroEL binds nucleotides but is inactive as a molecular chaperone. *J Biol Chem* 270: 20404–20409.
- Bukau B, Horwich AL (1998) The Hsp70 and Hsp60 chaperone machines. *Cell* 92: 351–366.
- Rye HS, Burston SG, Fenton WA, Beechem JM, Xu Z, et al. (1997) Distinct actions of cis and trans ATP within the double ring of the chaperonin GroEL. *Nature* 388: 792–798.
- Wang CY, Mayo MW, Korneluk RG, Goeddel DV, Baldwin AS, Jr. (1998) NF-kappaB antiapoptosis: induction of TRAF1 and TRAF2 and c-IAP1 and c-IAP2 to suppress caspase-8 activation. *Science* 281: 1680–1683.
- Kokoszka JE, Coskun P, Esposito LA, Wallace DC (2001) Increased mitochondrial oxidative stress in the Sod2 (+/-) mouse results in the age-related decline of mitochondrial function culminating in increased apoptosis. *Proc Natl Acad Sci U S A* 98: 2278–2283.
- Kamata H, Honda S, Maeda S, Chang L, Hirata H, et al. (2005) Reactive oxygen species promote TNFalpha-induced death and sustained JNK activation by inhibiting MAP kinase phosphatases. *Cell* 120: 649–661.
- Tobiume K, Matsuzawa A, Takahashi T, Nishitoh H, Morita K, et al. (2001) ASK1 is required for sustained activations of JNK/p38 MAP kinases and apoptosis. *EMBO Rep* 2: 222–228.
- Maeda S, Kamata H, Luo JL, Leffert H, Karin M (2005) IKKbeta couples hepatocyte death to cytokine-driven compensatory proliferation that promotes chemical hepatocarcinogenesis. *Cell* 121: 977–990.
- Wong GH, Elwell JH, Oberley LW, Goeddel DV (1989) Manganous superoxide dismutase is essential for cellular resistance to cytotoxicity of tumor necrosis factor. *Cell* 58: 923–931.
- Takeda K, Takeuchi O, Tsujimura T, Itami S, Adachi O, et al. (1999) Limb and skin abnormalities in mice lacking IKKalpha. *Science* 284: 313–316.
- Tanaka T, Ohkubo S, Tatsuno I, Prives C (2007) hCAS/CSE1L associates with chromatin and regulates expression of select p53 target genes. *Cell* 130: 638–650.
- Scheidereit C (2006) IkappaB kinase complexes: gateways to NF-kappaB activation and transcription. *Oncogene* 25: 6685–6705.
- Hoberg JE, Yeung F, Mayo MW (2004) SMRT derepression by the IkappaB kinase alpha: a prerequisite to NF-kappaB transcription and survival. *Mol Cell* 16: 245–255.

54. Boyle WJ, Simonet WS, Lacey DL (2003) Osteoclast differentiation and activation. *Nature* 423: 337–342.
55. Dai S, Hirayama T, Abbas S, Abu-Amer Y (2004) The IkappaB kinase (IKK) inhibitor, NEMO-binding domain peptide, blocks osteoclastogenesis and bone erosion in inflammatory arthritis. *J Biol Chem* 279: 37219–37222.
56. Chaisson ML, Branstetter DG, Derry JM, Armstrong AP, Tometsko ME, et al. (2004) Osteoclast differentiation is impaired in the absence of inhibitor of kappa B kinase alpha. *J Biol Chem* 279: 54841–54848.
57. Kobayashi K, Takahashi N, Jimi E, Udagawa N, Takami M, et al. (2000) Tumor necrosis factor alpha stimulates osteoclast differentiation by a mechanism independent of the ODF/RANKL-RANK interaction. *J Exp Med* 191: 275–286.
58. Otera H, Ohsakaya S, Nagaura Z, Ishihara N, Mihara K (2005) Export of mitochondrial AIF in response to proapoptotic stimuli depends on processing at the intermembrane space. *Embo J* 24: 1375–1386.
59. Susin SA, Lorenzo HK, Zamzami N, Marzo I, Snow BE, et al. (1999) Molecular characterization of mitochondrial apoptosis-inducing factor. *Nature* 397: 441–446.
60. Hegde R, Srinivasula SM, Zhang Z, Wassell R, Mukattash R, et al. (2002) Identification of Omi/HtrA2 as a mitochondrial apoptotic serine protease that disrupts inhibitor of apoptosis protein-caspase interaction. *J Biol Chem* 277: 432–438.
61. Suzuki Y, Imai Y, Nakayama H, Takahashi K, Takio K, et al. (2001) A serine protease, HtrA2, is released from the mitochondria and interacts with XIAP, inducing cell death. *Mol Cell* 8: 613–621.
62. Lai HC, Liu TJ, Ting CT, Yang JY, Huang L, et al. (2007) Regulation of IGF-I receptor signaling in diabetic cardiac muscle: dysregulation of cytosolic and mitochondria HSP60. *Am J Physiol Endocrinol Metab* 292: E292–297.
63. Gupta S, Knowlton AA (2002) Cytosolic heat shock protein 60, hypoxia, and apoptosis. *Circulation* 106: 2727–2733.
64. Jung Y, Kim H, Min SH, Rhee SG, Jeong W (2008) Dynein light chain LC8 negatively regulates NF-kappaB through the redox-dependent interaction with IkappaBalpha. *J Biol Chem* 283: 23863–23871.
65. Fujita T, Nolan GP, Ghosh S, Baltimore D (1992) Independent modes of transcriptional activation by the p50 and p65 subunits of NF-kappa B. *Genes Dev* 6: 775–787.
66. Makris C, Roberts JL, Karin M (2002) The carboxyl-terminal region of IkappaB kinase gamma (IKKgamma) is required for full IKK activation. *Mol Cell Biol* 22: 6573–6581.
67. Mercurio F, Zhu H, Murray BW, Shevchenko A, Bennett BL, et al. (1997) IKK-1 and IKK-2: cytokine-activated IkappaB kinases essential for NF-kappaB activation. *Science* 278: 860–866.
68. Jung MS, Jin DH, Chae HD, Kang S, Kim SC, et al. (2004) Bcl-xL and E1B-19K proteins inhibit p53-induced irreversible growth arrest and senescence by preventing reactive oxygen species-dependent p38 activation. *J Biol Chem* 279: 17765–17771.
69. Sanchez I, Hughes RT, Mayer BJ, Yee K, Woodgett JR, et al. (1994) Role of SAPK/ERK kinase-1 in the stress-activated pathway regulating transcription factor c-Jun. *Nature* 372: 794–798.
70. Chang TS, Cho CS, Park S, Yu S, Kang SW, et al. (2004) Peroxiredoxin III, a mitochondrion-specific peroxidase, regulates apoptotic signaling by mitochondria. *J Biol Chem* 279: 41975–41984.
71. Kang SW, Chae HZ, Seo MS, Kim K, Baines IC, et al. (1998) Mammalian peroxiredoxin isoforms can reduce hydrogen peroxide generated in response to growth factors and tumor necrosis factor-alpha. *J Biol Chem* 273: 6297–6302.